USGS
science for a changing world

An Analytical Method for Predicting Postwildfire Peak Discharges

Scientific Investigations Report 2011–5236

U.S. Department of the Interior
U.S. Geological Survey

Cover: Photograph by Thomas M. Trujillo, Los Alamos, New Mexico.

An Analytical Method for Predicting Postwildfire Peak Discharges

By John A. Moody

Scientific Investigations Report 2011–5236

U.S. Department of the Interior
U.S. Geological Survey

U.S. Department of the Interior
KEN SALAZAR, Secretary

U.S. Geological Survey
Marcia K. McNutt, Director

U.S. Geological Survey, Reston, Virginia: 2012

This and other USGS information products are available at http://store.usgs.gov/
U.S. Geological Survey
Box 25286, Denver Federal Center
Denver, CO 80225

To learn about the USGS and its information products visit http://www.usgs.gov/
1-888-ASK-USGS

Any use of trade, product, or firm names is for descriptive purposes only and does not imply endorsement by the U.S. Government.

Although this report is in the public domain, permission must be secured from the individual copyright owners to reproduce any copyrighted materials contained within this report.

Suggested citation:
Moody, J.A., 2012, An analytical method for predicting postwildfire peak discharges: U.S. Geological Survey Scientific Investigations Report 2011–5236, 36 p.

Contents

Figures

Tables

Abbreviations Used in This Report

<	less than
>	greater than
≥	greater than or equal to
ΔNBR	change in normalized burn ratio
Φ	hydraulic functional connectivity
C	modified runoff coefficient
CN	curve number
f	degrees of freedom; the number of independent values in a regression
I_{30}	maximum 30-minute rainfall intensity
I_{30}^{thres}	rainfall threshold for runoff generation
Q_u	unit peak discharge or peak discharge per unit drainage area
R^2	coefficient of determination is a statistical measure of the proportion of variability in a data set that is explained by a linear regression model with $R^2 = 0$ indicating no variance is explained by the model and $R^2 = 1$ all the variance is explained by the model.
se	standard error is the standard deviation of a set of N values normalized by square root of N.
USGS	U.S. Geological Survey

Units of Measure Used in This Report

ft	foot
$ft^3\ s^{-1}\ acre^{-1}$	cubic foot per second per acre
h	hour
in. h^{-1}	inches per hour
m	meter
mm	millimeter
mm h^{-1}	millimeters per hour
$m^3 s^{-1} km^{-2}$	cubic meters per second per square kilometer
s	second

Conversion Factors and Datums

Inch/Pound to SI

Multiply	By	To obtain
	Length	
inch (in.)	25.4	millimeter (mm)
foot (ft)	0.3048	meter (m)
mile (mi)	1.609	kilometer (km)
	Area	
acre	4,047	square meter (m^2)
acre	0.004047	square kilometer (km^2)
square mile (mi^2)	2.590	square kilometer (km^2)
	Flow rate	
foot per second (ft/s)	0.3048	meter per second (m/s)
cubic foot per second (ft^3/s)	0.02832	cubic meter per second (m^3/s)
cubic foot per second per square mile [$(ft^3/s)/mi^2$]	0.01093	cubic meter per second per square kilometer [$(m^3/s)/km^2$]
inch per hour (in./h)	0 .0254	meter per hour (m/h)

SI to Inch/Pound

Multiply	By	To obtain
	Length	
millimeter (mm)	0.03937	inch (in.)
meter (m)	3.281	foot (ft)
kilometer (km)	0.6214	mile (mi)
	Area	
square kilometer (km^2)	247.1	acre
square kilometer (km^2)	0.3861	square mile (mi^2)
	Volume	
cubic meter (m^3)	35.31	cubic foot (ft^3)
cubic meter (m^3)	1.308	cubic yard (yd^3)
	Flow rate	
cubic meter per second (m^3/s)	70.07	acre-foot per day (acre-ft/d)
meter per second (m/s)	3.281	foot per second (ft/s)
cubic meter per second (m^3/s)	35.31	cubic foot per second (ft^3/s)
cubic meter per second per square kilometer [$(m^3/s)/km^2$]	91.49	cubic foot per second per square mile [$(ft^3/s)/mi^2$]

Datums

Vertical coordinate information is referenced to the insert datum name (and abbreviation) here for instance, “North American Vertical Datum of 1988 (NAVD 88).”

Horizontal coordinate information is referenced to the insert datum name (and abbreviation) here for instance, “North American Datum of 1983 (NAD 83).”

Altitude, as used in this report, refers to distance above the vertical datum.

An Analytical Method for Predicting Postwildfire Peak Discharges

By John A. Moody

Abstract

An analytical method presented here that predicts postwildfire peak discharge was developed from analysis of paired rainfall and runoff measurements collected from selected burned basins. Data were collected from 19 mountainous basins burned by eight wildfires in different hydroclimatic regimes in the western United States (California, Colorado, Nevada, New Mexico, and South Dakota). Most of the data were collected for the year of the wildfire and for 3 to 4 years after the wildfire. These data provide some estimate of the changes with time of postwildfire peak discharges, which are known to be transient but have received little documentation. The only required inputs for the analytical method are the burned area and a quantitative measure of soil burn severity (change in the normalized burn ratio), which is derived from Landsat reflectance data and is available from either the U.S. Forest Service or the U.S. Geological Survey. The method predicts the postwildfire peak discharge per unit burned area for the year of a wildfire, the first year after a wildfire, and the second year after a wildfire. It can be used at three levels of information depending on the data available to the user; each level requires either more data or more processing of the data. Level 1 requires only the burned area. Level 2 requires the burned area and the basin average value of the change in the normalized burn ratio. Level 3 requires the burned area and the calculation of the hydraulic functional connectivity, which is a variable that incorporates the sequence of soil burn severity along hillslope flow paths within the burned basin.

Measurements indicate that the unit peak discharge response increases abruptly when the 30-minute maximum rainfall intensity is greater than about 5 millimeters per hour (0.2 inches per hour). This threshold may relate to a change in runoff generation from saturated-excess to infiltration-excess overland flow. The threshold value was about 7.6 millimeters per hour for the year of the wildfire and the first year after the wildfire, and it was about 11.1 millimeters per hour for the second year after the wildfire.

Introduction

A major concern after wildfires is predicting the hydrologic response of burned basins. Extreme floods and debris flows are common responses to substantial rainfall following wildfires. Postwildfire floods, however, are difficult to predict because necessary data on soil properties are lacking, in addition to the paucity of rainfall-runoff data for burned basins (Moody and others, 2008a). In general, two methods are used to estimate peak discharges by 71 percent of burn area emergency response specialists: the regression method, which is an adaptation of U.S. Geological Survey's regional regression equations, and the curve-number method developed by the Natural Resources Conservation Service (formerly Soil Conservation Service) (Foltz and others, 2009). Both methods were developed from data for unburned basins that contain perennial streams. In contrast, many streams within areas burned by wildfire are ephemeral, and heat from wildfire and combustion of vegetation can change soil properties and hydrologic response (Giovannini and others, 1988; DeBano, 2000; Doerr and others, 2000). The regression method requires regional regression equations for burned basins, but such equations do not exist and, therefore, the user must determine a modifier, which is the ratio of postwildfire to prewildfire runoff (Foltz and others, 2009). However, this ratio in essence requires knowing what one is trying to predict, that is, the postwildfire runoff. The curve-number method (Mockus, 1972; Foltz and others, 2009) predicts total runoff but not peak discharge. Thus, peak discharge must be estimated by applying an additional method (Mockus, 1949; Chow, 1964; Snider, 1972) or, commonly for larger basins, by using a numerical hydrograph routing method (Beven, 2001). Curve-number parameters (curve number (CN), initial abstraction, and maximum storage) were originally developed by using "ordered pairs" of data (rainstorms paired with floods that have the same recurrence interval) for unburned agricultural basins. However, in reality, an n-year-recurrence rainstorm (n = integer year such as 2, 5, 10, 50) may not produce an n-year-recurrence flood in an unburned basin, and it definitely

does not in a burned basin where a 2-year rainstorm might produce a flood with a 50-year or longer recurrence interval. A flood with a 50-year recurrence interval has a 2-percent probability of occurring in a given year. Recently some researchers have used "natural pairs" (rainstorms paired with the resulting floods), and so doing produces different curve-number parameters (Jiang, 2001; Woodward and others, 2003; Baltas and others, 2007, and R.H. Hawkins, University of Arizona, oral commun., 2002). At present, there are no clear guidelines for choosing postwildfire curve-number parameters (Foltz and others, 2009). To address the need for predictions of postwildfire peak discharges, available data and results from previous U.S. Geological Survey research activites were used to develop an analytical method that retains the cause-and-effect relation of rainfall and runoff.

Purpose and Scope

This report presents an analytical method for predicting postwildfire peak discharge for the first and second years after a wildfire; the method can be used by land and emergency managers for postwildfire assessment and response planning. It is based on natural pairs of rainstorm characteristics and peak discharges measured in 19 mountainous basins burned by wildfire that are located in various rainfall regimes in five western states (California, Colorado, Nevada, New Mexico, and South Dakota). The analytical method can be used to predict postwildfire peak discharges after any wildfire. In this report, predictions made by using this analytical method are compared with predictions made by using the curve-number method for five basins burned by the 2010 Fourmile Canyon fire near Boulder, Colo. These five basins and others were of special concern to the National Weather Service; the Urban Drainage and Flood Control District (Denver, Colo.); Boulder County, Colo.; and the City of Boulder, Colo., because of the potential for extreme flooding, debris flow, and loss of life. (Kurt Bauer, written commun., 4 March 2011).

Rainfall Regimes

Wildfires are common in several rainfall regimes in the United States. Various air-mass sources (Hirschboeck, 1991) produce four principal rainfall types (Kincer, 1919; Smith, 1994) in the western United States (Arizona, Pacific, Subpacific, and Plains, fig. 1). Each rainfall type (for example, Arizona) was further classified (Moody and Martin, 2009) into four rainfall regimes by using 2-year, 30-minute maximum rainfall intensities: low, 10–20 millimeters per hour (mm h^{-1}); medium, greater than (>) 20 to 36 mm h^{-1}; high, >36 to 52 mm h^{-1}; and extreme, >52 to 100 mm h^{-1} (low, 0.4 to 0.8 inches per hour (in. h^{-1}); medium, >0.8 to 1.4 in. h^{-1}); high, >1.4 to 2.0 in. h^{-1}; and extreme, >2.0 to 3.9 in. h^{-1}) providing a total of 10 rainfall regimes in the western United States.

Natural pairs of rainfall and postwildfire peak discharge data were compiled for sites within 5 of the 10 rainfall regimes (fig. 1). All wildfires were in mountainous terrain. The sites do not include sites of postwildfire floods from rain-on-snow events that are common within the Pacific-medium regime in the northwestern part of the United States and sometime within the Sub-Pacific-low and Plains-medium regimes in Idaho and western Montana. The sites (table 1) do include the Mediterranean-type climate common in southern California during the northern winter, which is generally characterized by long-duration, low-intensity frontal storms moving inland from the Pacific Ocean. Summer convective-storm regimes are generally characterized by short-duration, high-intensity rainfall (Plains-medium and Plains-high), which are common in some mountainous areas of the western United States.

Rain is commonly the driver of postwildfire floods. Unlike data derived from laboratory studies and rainfall simulation, the data in this report are not controlled but rather represent the natural variability of rainstorms that have substantial spatial and temporal variability (fig. 2). Spatially uniform rain is rare at the scale required to generate sufficient runoff to cause natural hazards. For example, 30-minute maximum rainfall intensity can range from a 2-year recurrence interval to a 100-year recurrence interval within short distances (fig. 2*A*).

An unresolved question is what temporal rain characteristics are physically appropriate to correlate with postwildfire peak discharges. This report uses 30-minute maximum intensity for the reasons below.

1. Storms generally have been found to produce about 80 percent of their rain in the first 30 minutes (Osborne and Renard, 1970; Miller and others, 1973, their table 12).

2. Storms in mountainous areas of western United States generally last less than 1 hour (Livingston and Minges, 1987; B. Glancy, National Oceanic and Atmospheric Administration, oral commun., 2011).

3. Thirty-minute rainfall amounts are used by some flash-flood prediction programs (Urban Drainage and Flood Control District (Denver, Colo.), 2011a).

4. The estimated time for water to travel from the most distant point of a basin to its outlet (time to concentration) averages about 22 minutes for the basins used in this report (table 1) and suggests that 30 minutes may be an approximation of the physically appropriate time scale.

Postwildfire response is a transient phenomenon. For any given year, and depending upon the climate, most postwildfire peak discharges are produced by small rainstorms (recurrence interval equal to or less than 1 year), a few peak discharges are produced by medium-size rainstorms (1- to 2-year recurrence interval), and usually at most one peak discharge is produced by a large rainstorm (2- to 50-year recurrence interval). Thus, it should be remembered throughout this report that the rain intensity–peak discharge relations are based on a paucity of natural pairs of rainstorms and peak discharges, especially for the largest peak discharges. Furthermore, grouping several years of data to increase the size of the statistical sample and

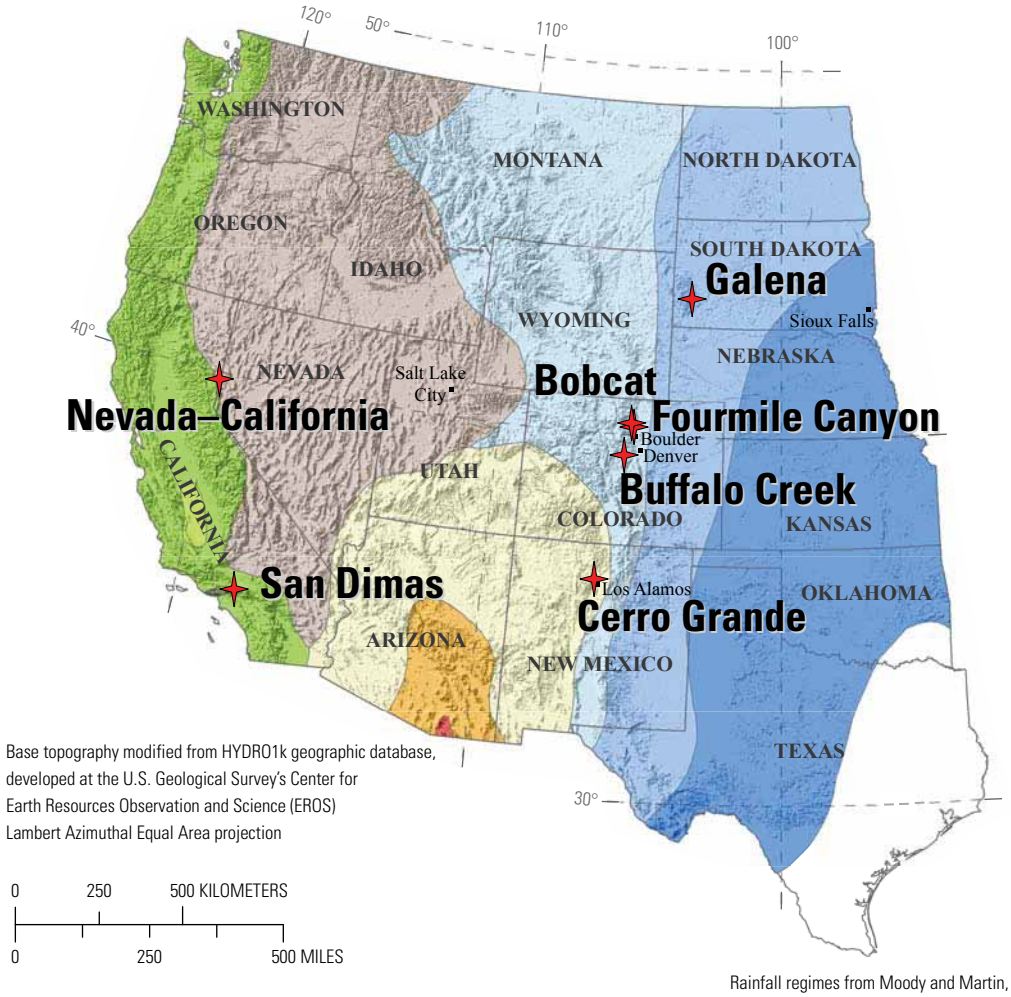

Figure 1. Location of wildfire sites within rainfall regimes of the western United States. (See Moody and Martin (2009) for description of rainfall regimes. (Pacific, high regime is partly hidden by symbol for San Dimas wildfire site.)

Table 1. Selected characteristics of burned basins studied in the western United States.

[km², square kilometer; min, minute; ≈, about equal to, %, percent; Calif., California; na, not available]

Fire and year[1]		Basin	Basin area		Basin relief or mean watershed slope	Estimate of time to concentration[2] (min)	Burned area			Source
			(km²)	(acre)			(%)	(km²)	(acre)	
San Dimas	1953	Fern, Upper East Fork, Wolfskill	5.5–6.2	1,360–1,530	0.14–0.18	25–37	≈100	5.5–6.2	1,360–1,530	San Dimas Staff, 1954
	1955	Wolfskill	6.2	1,530	0.15	37	≈100	6.2	1,530	Sinclair and Hamilton, 1955
	1960	Monroe and Volfe	3.0–3.5	740–866	0.11–0.13	22–23	≈100	3.0–3.5	740–866	Krammes and Rice, 1963
Nevada-Calif.	1960	Two unnamed basins	0.98–1.21	240–300	na	na	≈100	0.98–1.21	na	Copeland and Croft, 1962
Galena	1988	Bear Gulch	17.0	4,200	0.049	50	65	11.1	2,740	Moody and Martin, 2001a
Buffalo Creek	1996	Spring Creek	26.8	6,620	0.076	41	79	21.2	5,240	Moody and Martin, 2001a,b
Cerro Grand	2000	Rendija Canyon, 7 subbasins	0.25–0.85	62–210	0.0074–0.50	3.5–49	100	0.25–0.85	62–210	Moody and others, 2008
	2000	Pueblo Canyon	21.7	5,360	0.13	16	28	6.18	1,530	Reneau and Kuyumjian, 2004
Bobcat	2000	Bobcat Gulch	2.2	540	[3]0.32	17	98	2.2	540	Kunze and Stednick, 2006
	2000	Jug Gulch	3.9	960	[3]0.33	15	100	3.9	960	Kunze and Stednick, 2006

[1]See figure 1 for location of fires.

[2]Time to concentration estimated by using equation 10–3. p. 302, of Dunne and Leopold (1978); use these values only to compare basins shown in this table.

[3]Estimated from Kunze and Stednick (2006), their figure 1.

reduce variability has the underlying problem that soil properties and vegetation in the burned basins are changing with time such that the rain intensity–peak discharge relation may also be changing.

Data Used for the Analytical Method

Three types of data are used in this report: peak discharge, rain intensity, and soil burn severity. Peak discharges were measured by semidirect methods (such as pressure gages) or by indirect methods based on flood-stage high-water marks preserved along channels. Rain intensities were measured using digital or analog rainfall recorders. Analog records were digitized manually and then the data were analyzed. Rain intensities represent point measurements for various numbers of rain gages at various spacings. More details can be found in each of the references listed in the Peak Discharge and Rain Intensity section that follows. Soil burn severity was measured by remote-sensing reflectance instruments on satellites and is explained in more detail in the Soil Burn Severity section.

Peak Discharge and Rain Intensity

Peak discharge and rain intensity data, used in the analytical method presented here, were obtained from various rainfall regimes in mountainous terrain (fig. 1). The bulk of the data comes from relatively long-term postwildfire studies that lasted at least 3 to 4 years after the 1988 Galena fire (Moody and Martin, 2001a) in South Dakota, 1996 Buffalo Creek (Moody and Martin, 2001a,b) and 2000 Bobcat

A. **2 July 2001 rainstorm within Upper Rendija Canyon burned by the 2000 Cerro Grande fire near Los Alamos, New Mexico**

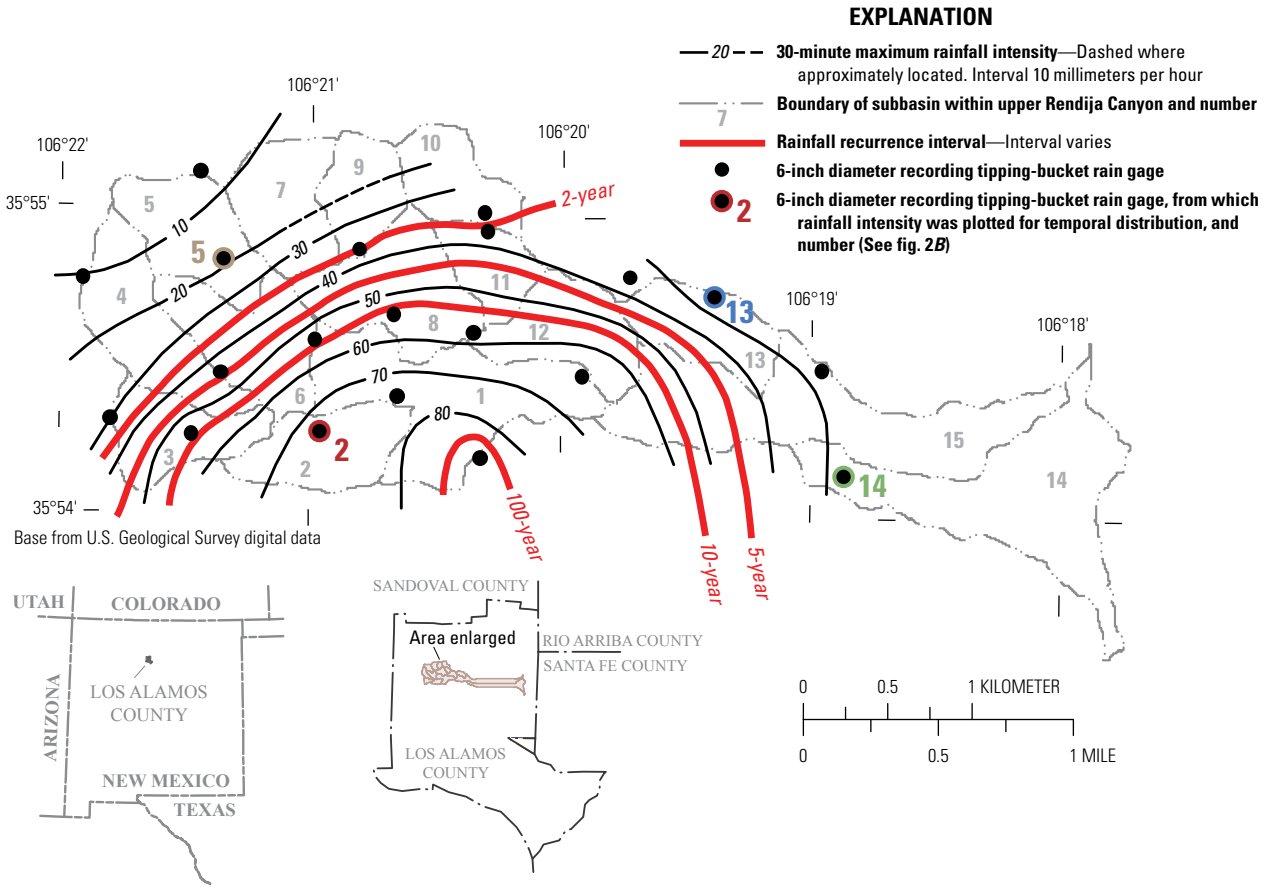

B. **Temporal distribution of rainfall intensity at four locations in the upper Rendija Canyon near Los Alamos, New Mexico**

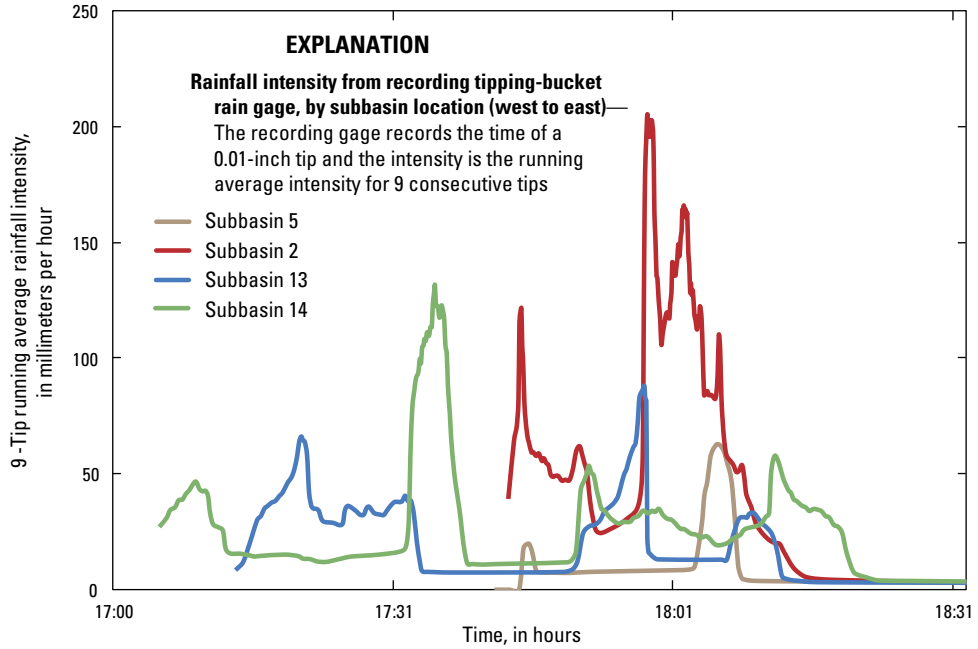

Figure 2. Upper Rendija Canyon. Spatial and temporal distribution of 30-minute, maximum rainfall intensity on 2 July 2001 following 2000 Cerro Grande fire near Los Alamos, New Mexico. *A*, Spatial distribution of rainfall intensity. *B*, Temporal distribution of rainfall in four subbasins.

(Kunze and Stednick, 2006) fires in Colorado, and the 2000 Cerro Grande fire (Reneau and Kuyumjian, 2004; Moody and others, 2008) in New Mexico. Additional data were compiled for California and Nevada wildfires from sources in published reports, which provided measurements of the peak discharge and sufficient rainfall measurements to calculate the 30-minute maximum rain intensity (San Dimas Staff, 1954; Sinclair and Hamilton, 1955; Copeland and Croft, 1962). Details of data collection methods and analysis can be found in each specific publication. Actual data values used in this report are listed in the appendix and grouped by years since the wildfire.

Soil Burn Severity

In fire ecology and management, "soil burn severity" is a widely used descriptive term, but it has different meanings depending upon the application. As applied to hydrologic response, soil burn severity assumes that changes in substrate (litter, duff, and mineral soil) and vegetation (tree canopy, understory, shrubs, herbs, and grasses) indicate the magnitude of the conductive and radiant heat impulse into the soil. This magnitude influences postwildfire runoff. Soil burn severity can be quantified as the change in the normalized burn ratio, ΔNBR. Values of ΔNBR are commonly classified as low, moderate, and high to produce the burned area reflectance classification (Parson and others, 2010). The normalized burn ratio is derived from remote sensing measurements of earth radiation (Landsat thematic mapper and Landsat ETM+ data); it is available from the U.S. Department of Agriculture's Forest Service Remote Sensing Applications center in Salt Lake City, Utah, and from the U.S. Geological Survey (USGS) Center for Earth Resources Observation and Science in Sioux Falls, S. Dak., for specific wildfires (Parsons and others, 2010). Raw digital values for Landsat spectral band 4 (R_4) and band 7 (R_7) are converted to radiance and then to at-satellite reflectance before computing the normalized burn ratio (NBR) (Key and Benson, 2004):

$$NBR = 1000(R_4 - R_7) / (R_4 + R_7). \quad (1)$$

The ratio represents a magnitude of change detected from two spectral bands sensitive to the effects of wildfire. Band 4 in the near infrared band (wavelength=0.76–0.90×10^{-6} m) measures the reflected radiation from vegetation (which typically decreases as a consequence of wildfire). Band 7 in the short-infrared band (wavelength=2.08–2.35×10^{-6} m) measures the reflected radiation from bare soil (which typically increases as a consequence of wildfire). ΔNBR is calculated as the prewildfire value of NBR minus the postwildfire value. Values can range from as low as −1,000 in unburned patches to as high as +1,000 in severely burned patches (see fig. 3 for typical basin-average values).

Hydraulic Functional Connectivity

Basin average values of ΔNBR do not retain any information about the pattern of soil burn severity. However, along hydrological flow paths this pattern may be critical in determining the amount of water reaching a channel or passing downstream along a channel within a burned basin. Thus, the flow or discharge down the hillslope may depend on the connectivity or spatial sequence of soil burn severity associated with each pixel i, ΔNBR_i along a flow path, in which sequence those pixels closest to the channel have a greater weight. For this reason, hydraulic functional connectivity was defined to quantify the hydrological function of the sequence of soil burn severity along a hillslope flow path, j, composed of k connected pixels (Moody and others, 2008a). Hydraulic functional connectivity, Φ_j, is dimensionless and is computed using the following equation:

$$\Phi_j = \frac{\sum_{i=1}^{k} \alpha_{ij} \Delta NBR_{ij}}{\alpha}, \quad (2)$$

where α_{ij} is a weighting factor for ΔNBR_i equal to the uphill contributing area to pixel i in flow path j, and α is the area of one pixel. To illustrate the importance of the sequence of pixels encountered by water flowing down a hillslope flow path, a simple hypothetical flow path can be assumed with a pixel area equal to 1 and values of the soil burn severity, ΔNBR_i, for a 4-pixel hillslope flow path equal to 700, 500, 300, and 100 (fig. 4). For this sequence of soil burn severity, the value of Φ_j equals 750, but if the downhill sequence is reversed with the most severely burned pixel closest to the channel, the hydraulic functional connectivity, Φ_j, is 1,250. The basin average hydraulic functional connectivity, Φ, is the average of a set of random hillslope flow paths:

$$\Phi = \frac{1}{N} \sum_{j=1}^{N} \Phi_j \quad (3)$$

where N is the number of hillslope flow paths in a subbasin. At the pixel scale (30×30 m), determined by the Landsat imagery, it is impossible to resolve the detailed drainage network on hillslopes, but the pattern of soil burn severity is assumed to be imprinted onto the drainage network so that the hydraulic functional connectivity provides a first-order estimate of the spatial changes in soil burn severity along a hillslope flow path.

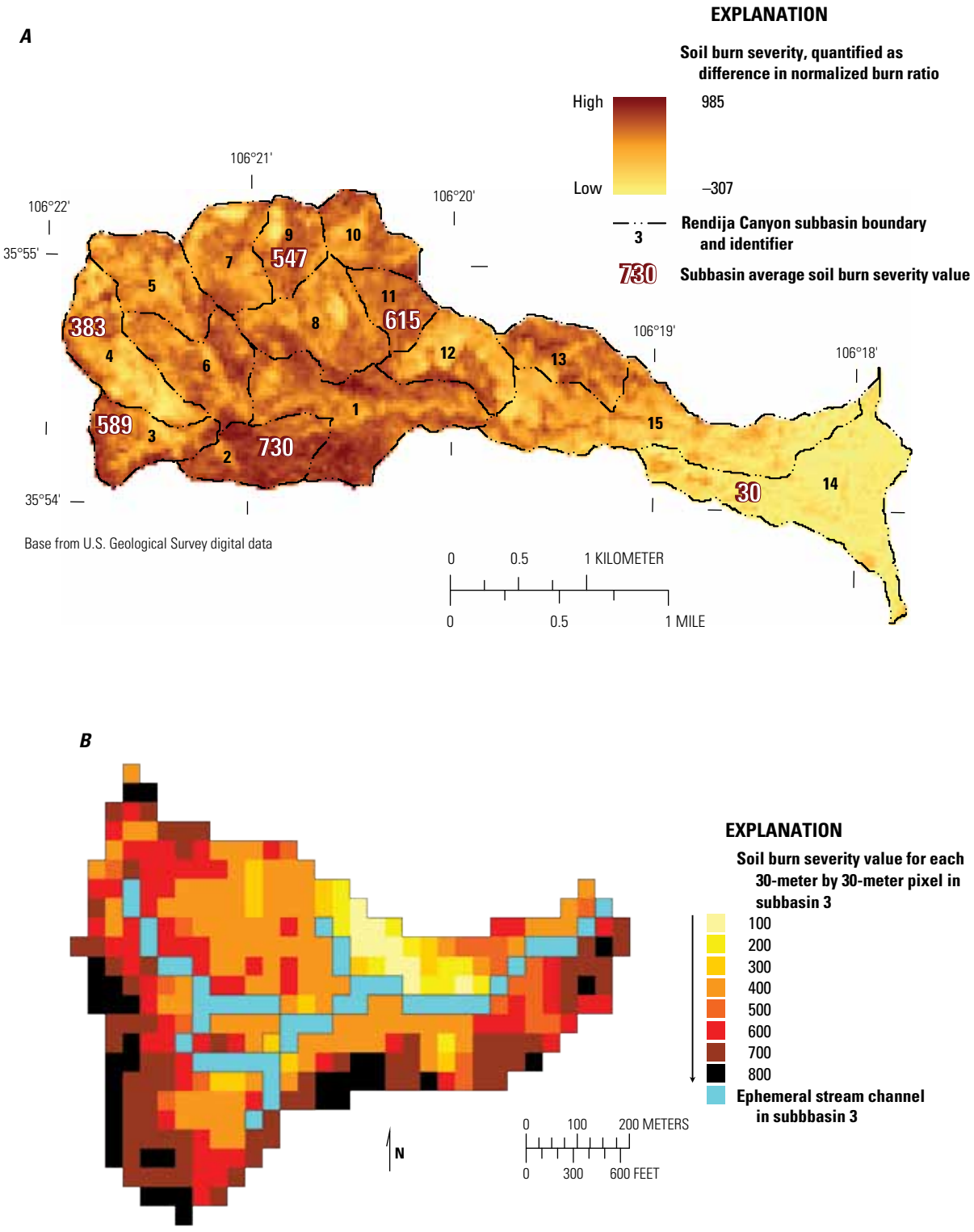

Figure 3. Values of ΔNBR (change in normalized burn ratio) in Rendija Canyon, New Mexico. *A*, Values of ΔNBR in selected subbasins burned by the 2000 Cerro Grande fire, near Los Alamos, New Mexico. *B*, Values of ΔNBR for each pixel in subbasin 3 in part *A*.

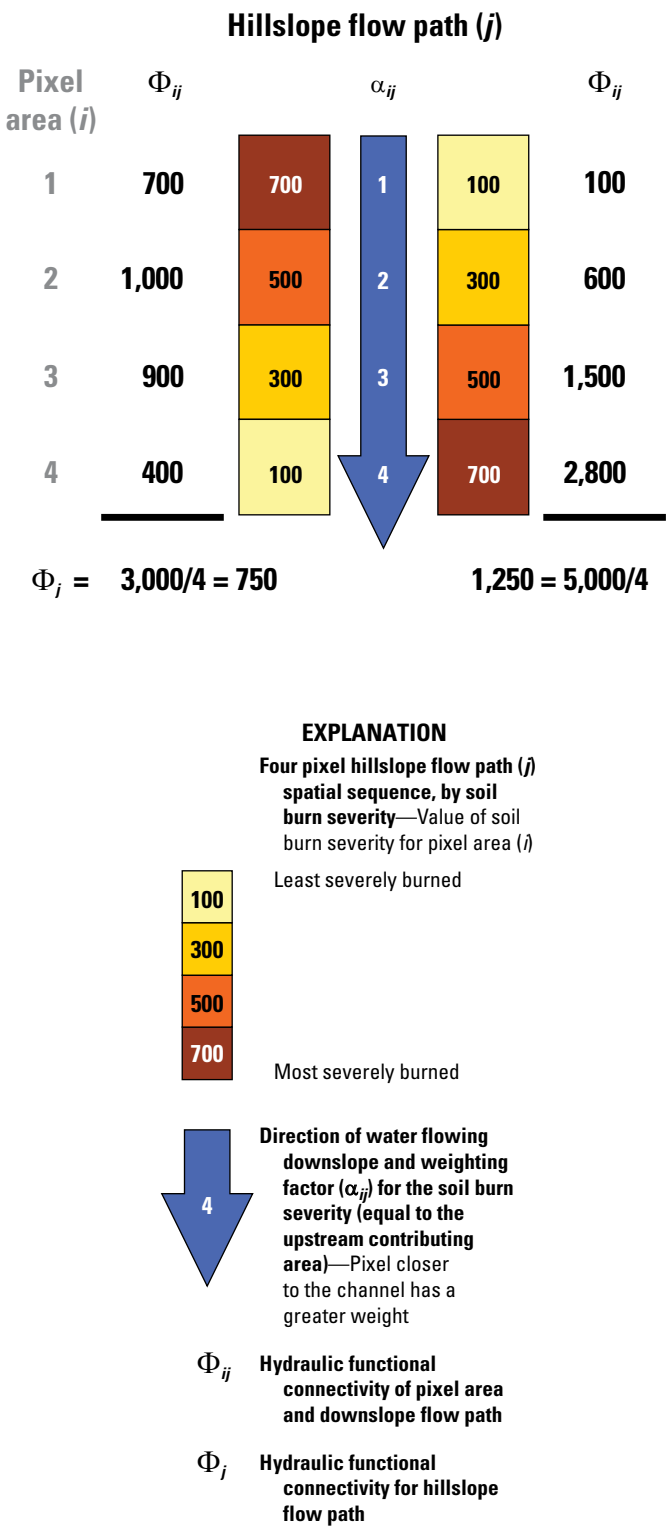

Figure 4. Hydraulic functional connectivity computed for a hillslope flow path *j* with two hypothetical sequences of ΔNBR (change in normalized burn ratio). See text for a more-detailed explanation.

Levels of Data Requirements

The analytical method can be used at three different levels. Each higher level requires additional data or additional data processing. Level 1 requires only an estimate of the area that contributes to the runoff. However, the actual area contributing to overland flow is usually unknown. It may expand and contract in space controlled by a precipitation rate exceeding infiltration rate resulting in infiltration-excess overland flow (Horton, 1933), or it may expand and contract in time by exhausting subsurface storage resulting in saturation-excess overland flow (Dunne and Black, 1970). For further explanation of these two distinct processes, see Chorley (1978) and Beven and Kirkby (1979). Because of these complications in determining contributing area, the entire basin area is commonly used as the contributing area, which tends to underestimate the unit peak discharge (discharge per unit contributing area). In this report the total burned area, usually less than the basin area, is used as the contributing area, which still may underestimate the unit peak discharge in some cases. Level 2 requires the burned area and the basin-averaged ΔNBR. Level 3 requires the burned area and the basin-averaged hydraulic functional connectivity, Φ, given by equation 3 in the previous section.

Analytical Method for Predicting Postwildfire Peak Discharges

Rain-intensity–peak-discharge relations are discussed for each basin burned by specific wildfires (table 1) to provide some insight into the entire data set. The data are then grouped, and more-general empirical relations are discussed for the first year and second year after a wildfire because, in general, land and emergency managers are most concerned about these two years. Those readers who are interested in the general empirical relations used by the analytical method for predicting the postwildfire peak discharge may want to skip to the following section below, General Rain-Intensity–Peak-Discharge Relations.

Individual Rain-Intensity–Peak-Discharge Relations

Data for each year since a wildfire are presented separately. In some cases, data were insufficient to justify computing a regression equation. In general, little or no hydrologic response was produced by 30-minute maximum rain intensities, I_{30} (mm h^{-1}; in. h^{-1}) less than 5 mm h^{-1} (0.2 in. h^{-1}). Therefore, the data for each wildfire were grouped as I_{30} greater than or equal to($\geq$)5 mm h^{-1} and as I_{30} less than ($<$5) mm h^{-1}. Because unit peak discharges may differ by 6 orders of magnitude, data are presented in log-log plots in order to show small values as well as large ones. Values of

I_{30}, in contrast, differ by only about 1 order of magnitude, which indicates the extreme sensitivity of postwildfire peak discharge to rain intensity. Unit peak discharges were not log-transformed to determine the rain-intensity–peak-discharge relations. Least-squares linear regression (Helsel and Hirsch, 1992) was used to determine relations between unit peak discharge, Q_u ($m^3\ s^{-1}\ km^{-2}$; $ft^3\ s^{-1}\ acre^{-1}$) and I_{30}. These linear relations appear as curved lines on a log-log plot and have the form

$$Q_u = C(I_{30} - I_{30}^{thres}) \quad (4)$$

where C is referred to in this report as the modified runoff coefficient ($m^3\ s^{-1}\ km^{-2}\ mm^{-1}\ h$; $ft^3\ s^{-1}\ acre^{-1} in.^{-1}\ h$; or dimensionless), and I_{30}^{thres} (mm h^{-1}; in. h^{-1}) can be interpreted as a threshold of rain intensity for runoff generation. Normally a runoff coefficient is the ratio of the unit peak discharge divided by the rain intensity and by conservation of mass must be less than or equal to –1. However, the modified runoff coefficient, C, can be greater than –1, because the value of I_{30}^{thres} is subtracted from the actual rain intensity producing what could be considered as an effective rain intensity ($I_{30} - I_{30}^{thres}$).

1996 Buffalo Creek Fire—Spring Creek, Colorado

Rain-intensity–peak-discharge relations for Spring Creek basin changed with time after the wildfire. Only one measurement was made in 1996 (12 July 1996) (fig. 5, yellow circle). This storm released an estimated 1-hour rainfall of 110 mm (Jarrett, 2001), which produced a major flood with an indirect discharge measurement of 510 $m^3\ s^{-1}$ (18,000 $ft^3\ s^{-1}$) and a value of the unit peak discharge, Q_u, equal to 24 $m^3\ s^{-1}\ km^{-2}$ (3.4 $ft^3\ s^{-1}\ acre^{-1}$) (Moody and Martin, 2001b). Spring Creek, a perennial stream flowing within a fractured granitic batholith landscape, has a quasisteady base flow. It responded to small values of $I_{30} < 5$ mm h^{-1}, which suggests that the runoff was probably saturated-excess overland flow arising from a narrow area immediately adjacent to the stream channel. Tributaries within the basin, however, are ephemeral, and water is usually below but close to the streambed. The modified runoff coefficient C decreased with increasing time after the wildfire from 0.11 to 0.00074 $m^3\ s^{-1}\ km^{-2}\ mm^{-1}\ h$ (0.40 to 0.0027 $ft^3\ s^{-1}\ acre^{-1}\ in.^{-1}\ h$) (fig. 5), or in dimensionless form, from 0.031 to 0.00021. By the 3d and 4th year after the wildfire, less of the variance is explained by the linear regression (see fig. 5 and values of R^2). The threshold I_{30}^{thres} was essentially constant (8.6 mm h^{-1}; 0.39 in. h^{-1}) for the first 2 years and was more variable for the 3d and 4th year on the basis of R^2 values. The rapid hydrologic response of the unit peak-discharge values in the neighborhood of I_{30}=5 mm h^{-1} (fig. 5) suggests that runoff may change from saturation-excess overland flow (I_{30}<5 mm h^{-1}) to infiltration-excess overland flow (I_{30}>5 mm h^{-1}).

2000 Cerro Grande Fire—Rendija Canyon, New Mexico

Rain intensity-peak discharge relations for Rendija Canyon also changed with time after the wildfire. Unlike Spring Creek, the most intense rainstorm was not during the year of the wildfire (2000), but a year later on 2 July 2001 (fig. 2). Such a lag time is common, and the largest rainfall and flood may occur more than 2 years after a wildfire (Robert Jarrett, USGS, written commun., 2011). Only four pairs of rainfall-runoff measurements were made in 2000 (fig. 6), and thus the regression relation has more uncertainty (R^2=0.28). Rain-intensity–peak-discharge data pairs were measured in seven subbasins (fig. 3*A*, those subbasins with subbasin-average ΔNBR values). All subbasins had ephemeral streams, as did the main channels of Upper Rendija Canyon. One measurement represents the third largest unit peak discharge (11.3 $m^3\ s^{-1}\ km^{-2}$; 1.6 $ft^3\ s^{-1}\ acre^{-1}$) in this report. The modified runoff coefficient, C, decreased from 0.56 $m^3\ s^{-1}\ km^{-2}\ mm^{-1}\ h$ (2.0 $ft^3\ s^{-1}\ acre^{-1}\ in.^{-1}\ h$) in year 2000 to 0.061 $m^3\ s^{-1}\ km^{-2}\ mm^{-1}\ h$ (0.22 $ft^3\ s^{-1}\ acre^{-1}\ in.^{-1}\ h$) in year 2002, and I_{30}^{thres} ranged from 7.2 to 12 mm h^{-1}(0. 0.28 to 0.47 in. h^{-1}). The hydrologic response was associated with high-intensity rain, $I_{30} \geq 5$ mm h^{-1} (fig. 6), and it suggests that, in contrast with Spring Creek, probably only the infiltration-excess process produced the runoff measured in Rendija Canyon. For $I_{30} < 5$ mm h^{-1} rain percolated into the stream bed, was absorbed by porous volcanic bedrock (Moody and others, 2008b), and produced no discharge. This example illustrates the initial abstraction concept used in the curve-number method. Numerous "no discharge" responses were detected during rainstorms in 2000–2002. The average value of I_{30} corresponding with no discharge was 7.7 mm h^{-1} (0.30 in. h^{-1}), which is within the range of I_{30}^{thres} values determined from the 2000–2002 rain intensity-peak discharge relations (fig. 6).

2000 Cerro Grande Fire—Pueblo Canyon, New Mexico

Pueblo Canyon is adjacent to Rendija Canyon on the edge of a volcanic caldera (Moody and others, 2008b), and it too has ephemeral channels during most of the year. Again rainfall-runoff data are lacking for 2000, the year of the wildfire (fig. 7). No rainstorm produced a measured value of I_{30} >17 mm h^{-1} (0.67 in. h^{-1}). Regression equations for the years after 2000 indicate a decrease in the modified runoff coefficient with time since the wildfire, and values of I_{30}^{thres} were similar to those for Rendija Canyon; they ranged from 7.1 to 12 mm h^{-1} (0.28–0.47 in. h^{-1}).

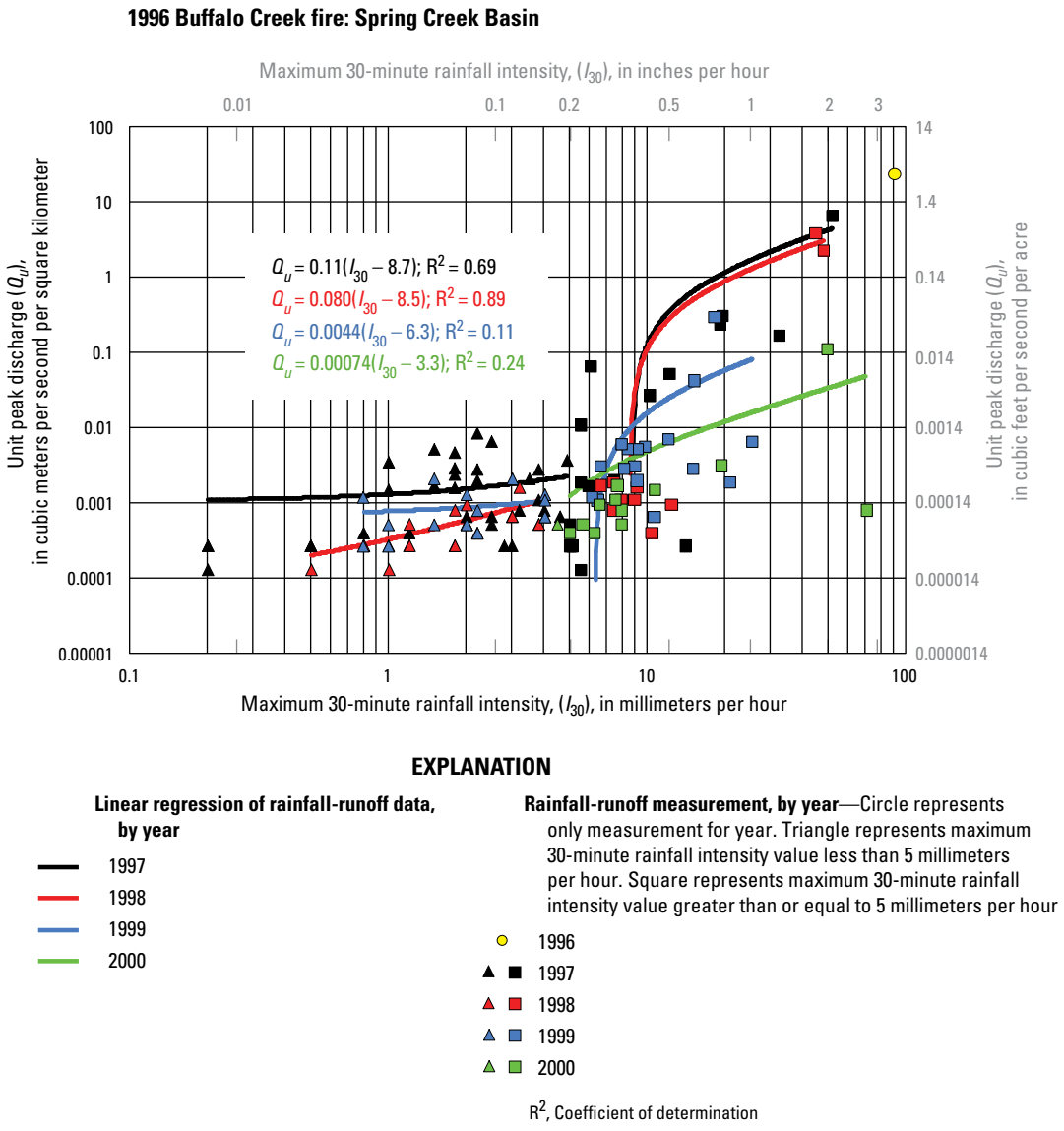

Figure 5. 1996 Buffalo Creek fire—Spring Creek Basin. Relation between rain intensity and unit peak discharge in Spring Creek, Colorado.

2000 Bobcat Fire—Bobcat and Jug Gulches, Colorado

The rain-intensity–peak-discharge relation for these two basins also changed with time since the wildfire. However, because of a major drought that had started by 2000 in some places and peaked in 2002 throughout most of Colorado (Moody and others, 2007), only one data pair was measured in 2002 (fig. 8). These basins, which were cut into tonalite and metasedimentary rocks (Kunze and Stednick, 2006), had ephemeral streams with no measured response (see fig. 8), for I_{30} <8 mm h^{-1} (0.31 in. h^{-1}). The estimates of I_{30}^{thres} from the regression analysis gave values of 9.9 and 11 mm h^{-1} (0.39 and 0.43 in. h^{-1}, respectively).

1988 Galena Fire—Bear Gulch, South Dakota

The generally downward trend of the modified runoff coefficient with time since the wildfire was less clear in data from Bear Gulch. Bear Gulch is a perennial stream, like Spring Creek; it showed, primarily in 1990 (fig. 9), a similar possible saturated-excess response for I_{30} <5 mm h^{-1}. For an unknown reason, data for the second year (1990) after the wildfire were more scattered (R^2=0.16) than data for other basins discussed above. However, regression equations for the first and third years were much better (R^2=0.85 and 0.83 respectively), and the modified runoff coefficient definitely decreased. Estimates of I_{30}^{thres} had the largest range (2.7–11 mm h^{-1} or 0.11–0.43 in. h^{-1}) of all the data sets.

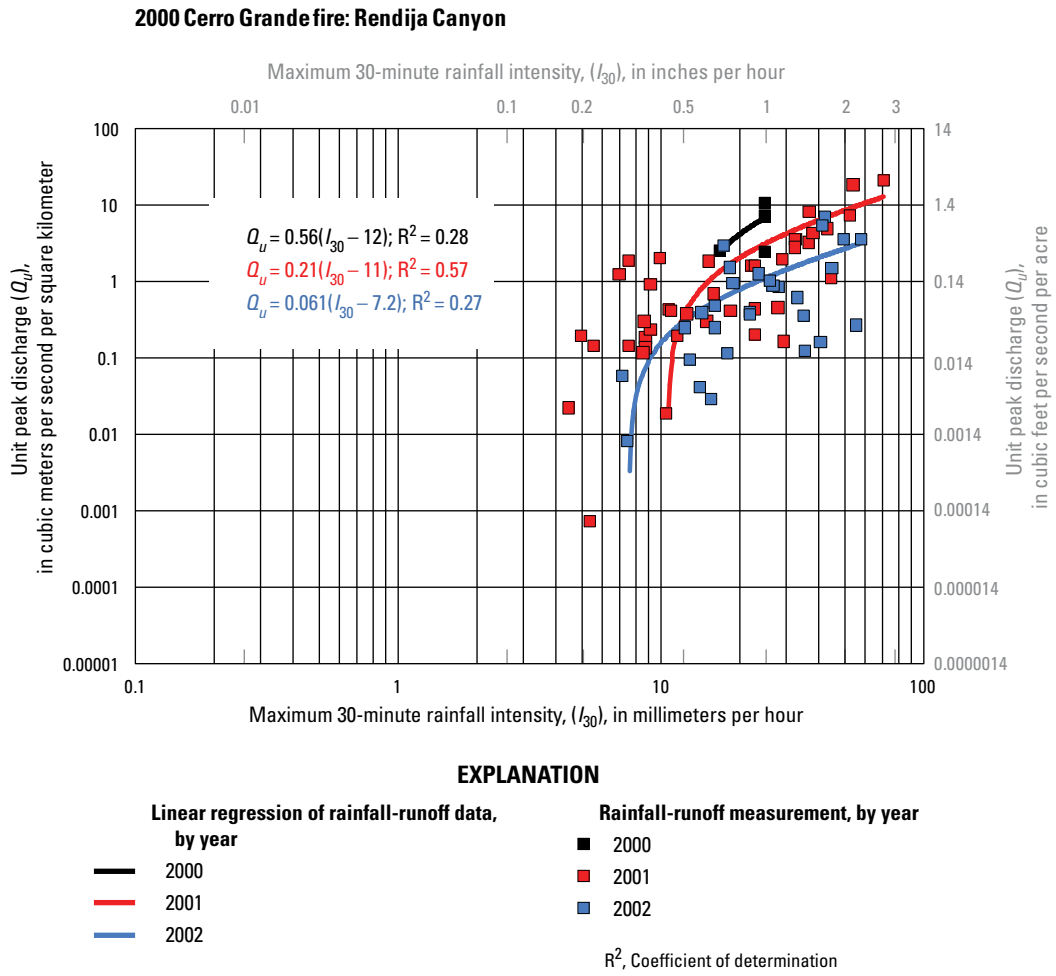

Figure 6. 2000 Cerro Grande fire—Rendija Canyon. Relation between rain intensity and unit peak discharge, Rendija Canyon, New Mexico.

Nevada and California Fires

Data extracted from the literature (San Dimas Staff, 1954; Sinclair and Hamilton, 1955; Copeland and Croft, 1962) that had sufficient information to determine the 30-minute maximum rainfall intensity were sparse and therefore grouped for Nevada-California fires. Most of these data were from basins underlain by metamorphic rocks in the San Dimas Experimental Forest in the San Gabriel Mountains of southern California. Within these data was the largest unit peak discharge, 32.7 $m^3\ s^{-1}\ km^{-2}$ or 4.7 $ft^3\ s^{-1}\ acre^{-1}$ (fig. 9), of all basins studied for this report. These data are selective in the sense that they represent the most noteworthy peak discharges and hence were reported in the literature. The lowest I_{30} was 18.8 mm h^{-1} (0.74 in. h^{-1}), but there were likely smaller rain intensities that were not reported.

Modified Runoff Coefficient

Each data set discussed above distinctly showed a general decrease in the modified runoff coefficient with time since the wildfire. Thus, all data sets were combined to provide an empirical equation that is applicable to several rainfall regimes (fig. 10):

$$C = 0.42e^{-1.3\Delta t};\ R^2{=}0.65 \qquad (5)$$

where Δt is the time in years since the wildfire and e is the mathematical constant (~2.718…). Some measurements of C were made less than a year after the wildfire. Although these measurements add some support to the general trend, the values of C ranged widely, from 0.12 to 0.56 $m^3\ s^{-1}\ km^{-2}\ mm^{-1}\ h$, whereas values for the first year after the wildfire

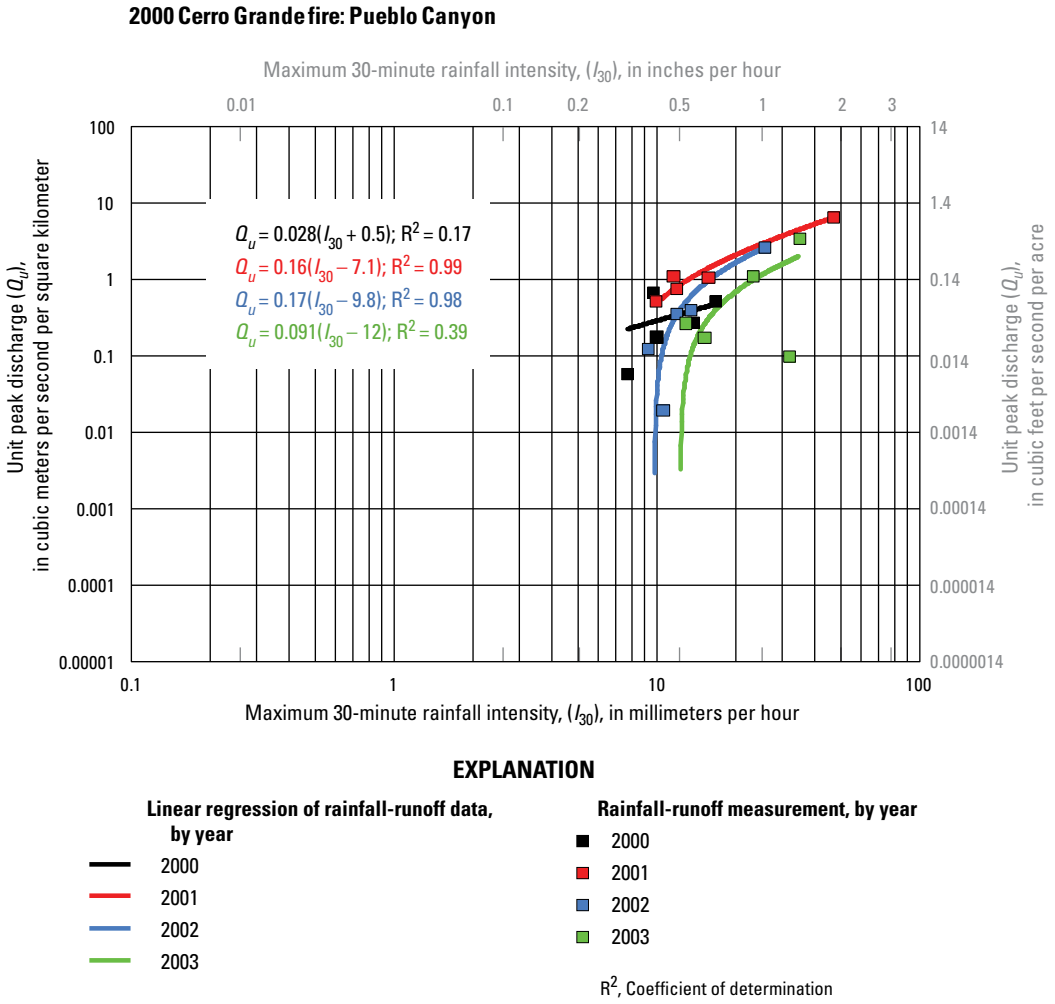

Figure 7. 2000 Cerro Grande fire—Pueblo Canyon. Relation between rain intensity and unit peak discharge, Pueblo Canyon, New Mexico.

varied much less. Predicting the postwildfire peak discharges for the year of the wildfire and for the first and second years after the wildfire is of prime concern for land and emergency managers. Thus, the equations for predicting the postwildfire peak discharge using the analytical method were developed separately for first year data and second year data. These two groups of data have the most data pairs and will be the most reliable. Postwildfire peak discharges for the year of the wildfire can be estimated using values from the first year and perhaps adjusted by using empirical equation 5, with the caveat that the estimates will be much more uncertain. However, one must keep in mind the large variability of rain intensity, which can produce substantial floods more than 2 years after a wildfire.

General Rain-Intensity–Peak-Discharge Relations

All data pairs for the year of a wildfire and for the first year after a wildfire were used to develop a general empirical relation between rain intensity, I_{30}, and the unit peak discharge, Q_u. This data set represents 19 basins within areas burned by eight wildfires (fig. 11). Unit peak discharge spans 6 orders of magnitude whereas the rain intensity spans only about 1 order of magnitude. A rain-intensity–peak-discharge relation could not be developed for data pairs with I_{30} <5 mm h^{-1} because the flow probably is generated by the saturation-excess, which depends on initial unsaturated storage and not on rain

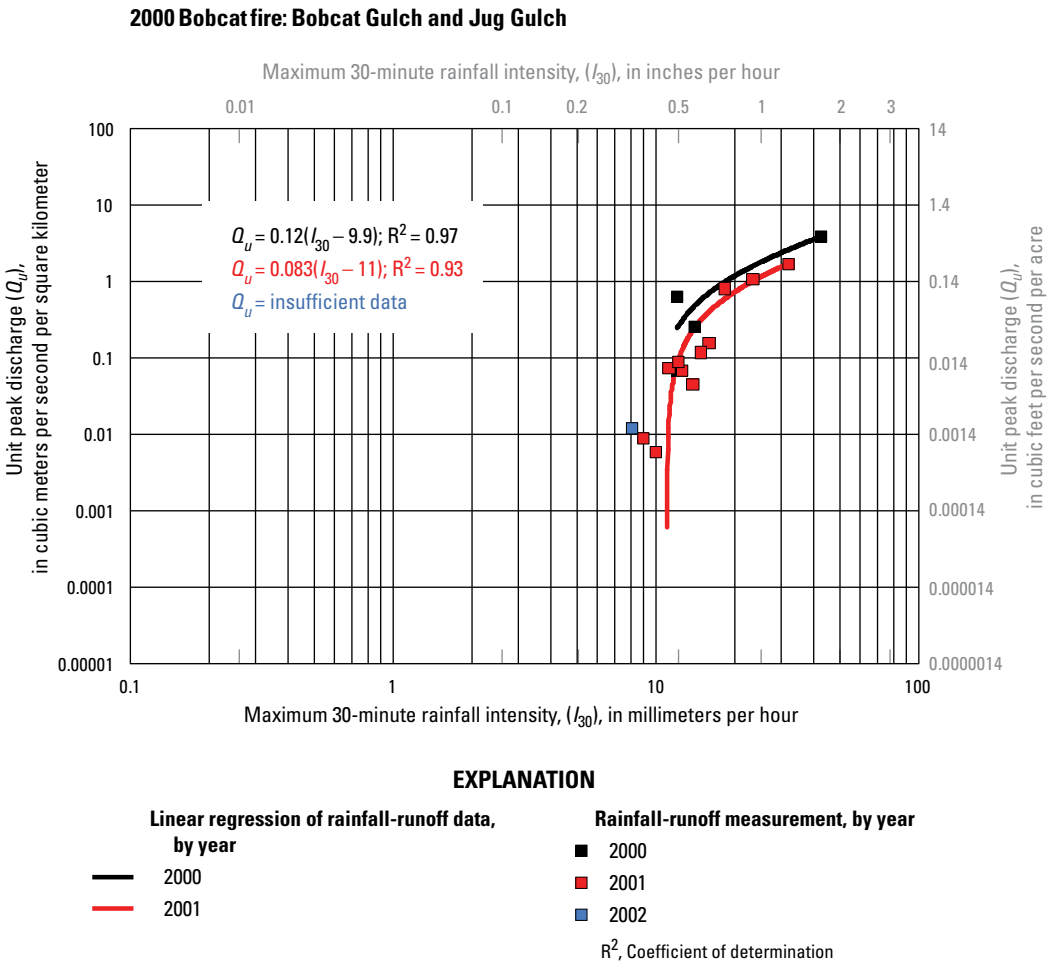

Figure 8. 2000 Bobcat fire—Bobcat Gulch and Jug Gulch. Relation between rain intensity and unit peak discharge, Bobcat and Jug Gulches, Colorado.

intensities. For example, the linear regression for the Spring Creek data and Bear Gulch (solid blue circles, fig. 11) had R^2 values <0.02 suggesting the absence of a relation between rain intensity and peak discharge.

The initial linear, empirical equation based on all the data for $I_{30} \geq 5$ mm h^{-1} is as follows:

$$Q_u = C(I_{30} - I_{30}^{thres}), \quad (6a)$$

or, in terms of the peak discharge Q [m^3 s^{-1}],

$$Q = C(I_{30} - I_{30}^{thres})A, \quad (6b)$$

where C=0.24 m^3 s^{-1} km^{-2} mm^{-1} h and I_{30}^{thres}=12 mm h^{-1}, and A [km^{-2}] is the contributing or burned area. The variability about this regression line (R^2=0.70; degrees of freedom=105) is approximately 1–2 orders of magnitude for Q_u and I_{30} at their largest values, but it is greater for smaller values of Q_u and I_{30}. The variability in the relation derives from the uncertainties of measuring peak discharges for water that is debris laden, is turbulent, and commonly has large surface waves (as shown on the cover of this report). It also derives from the spatial and temporal variability of rain (illustrated in fig. 2), which introduces uncertainty in the unknown value of the actual contributing area. Some idea of the uncertainty of rain intensities and unit peak discharges can be found in Moody and others (2008; fig. 3, a linear-linear plot), which corresponds with figure 6 (a log-log plot) in this report. The appendix has additional more-detailed regression statistics for equation 6. Another source of variability is different values of soil burn severity for each data pair.

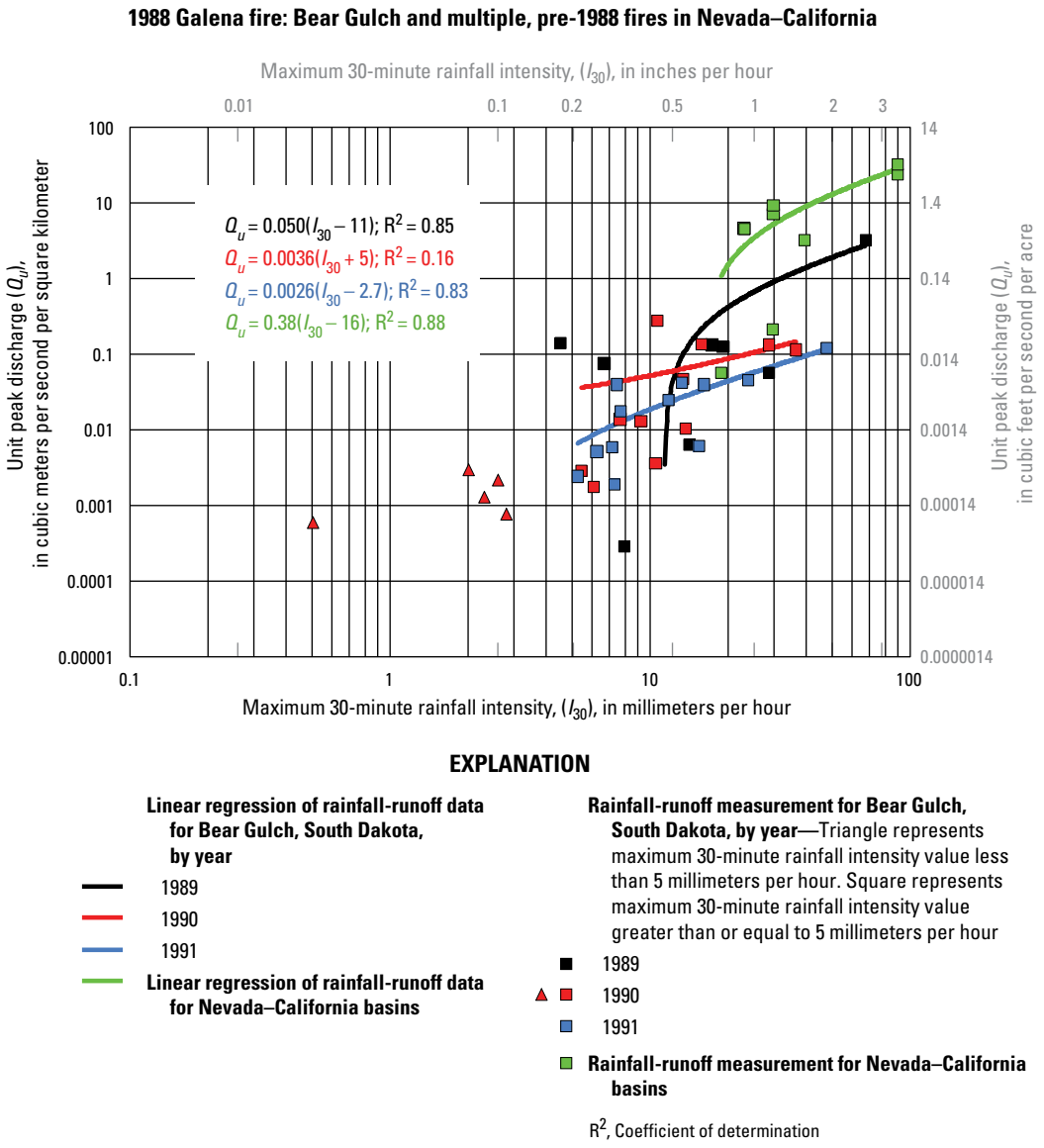

Figure 9. 2000 Galena fire—Bear Gulch and many pre-1988 fires—Nevada and California. Relation between rain intensity and unit peak discharge, Bear Gulch, South Dakota, and eight basins in California and Nevada.

The variability caused by different soil burn severities was controlled by using only those four basins with essentially the same soil burn severity, ΔNBR (581±5 percent) and recomputing the linear regression. These data were available only for Rendija Canyon (solid red triangles, fig. 11); the resulting linear, empirical equation has the same form as equations 6a and 6b,

$$Q_u = C(I_{30} - I_{30}^{thres}), \tag{7a}$$

or in terms of the peak discharge Q [$m^3\ s^{-1}$],

$$Q = C(I_{30} - I_{30}^{thres})A, \tag{7b}$$

where C, the modified runoff coefficient, is a function of the soil burn severity and has the value 0.14 $m^3\ s^{-1}\ km^{-2}\ mm^{-1}\ h$ for ΔNBR=581; I_{30}^{thres}=7.6 mm h^{-1}. Controlling the soil burn severity only slightly increases the explained variance (R^2=0.72; f=29) about the regression line (red line, fig.11) because the degrees of freedom are substantially fewer in this subset of the data; however, equations 6 and 7 are nearly the same (see appendix for more detailed regression statistics). Any of the equations 6a, 6b, 7a, and 7b can be used in level 1 analysis

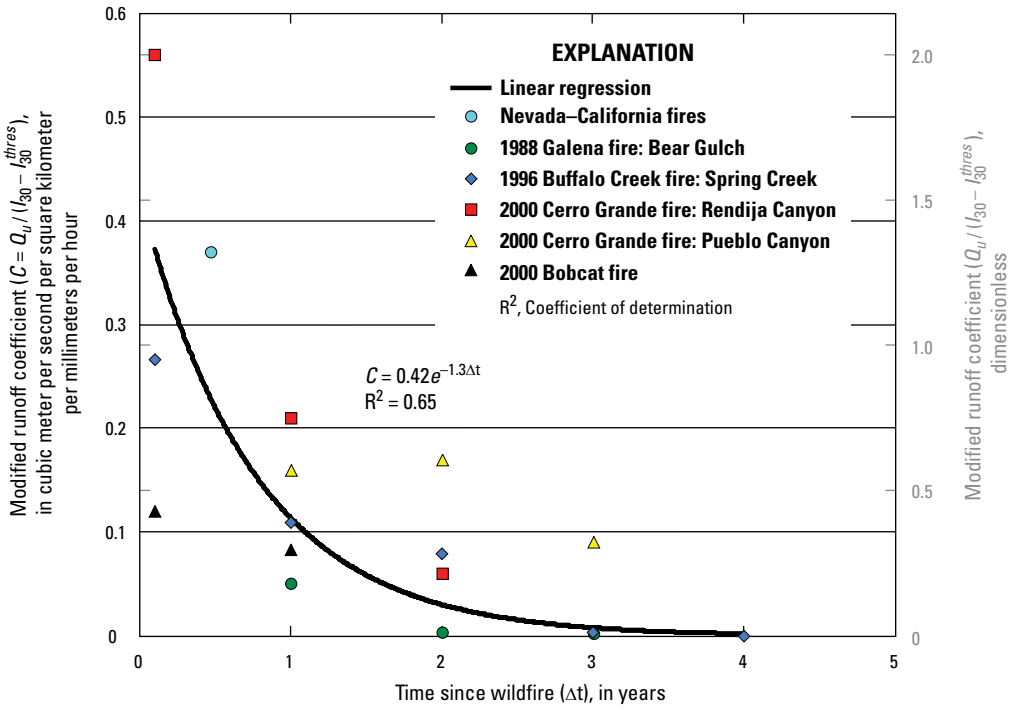

Figure 10. Dependence of modified runoff coefficient, *C*, on time since wildfire.

to estimate the postwildfire unit peak discharge or the peak discharges, if the burned area, *A*, is known and by selecting the value of I_{30} for a desired rainstorm recurrence interval. Additionally, these predictions of postwildfire peak discharge can be further refined by determining the dependence of *C* on Δ*NBR*.

Dependence of Modified Runoff Coefficient on Soil Burn Severity

The dependence of the modified runoff coefficient on soil burn severity decreases with time since a wildfire (fig. 12). There appears to be a corresponding increase in I_{30}^{thres} from 7.6 mm h^{-1} (0.30 in. h^{-1}) during the first year to 11.1 mm h^{-1} (0.44 in. h^{-1}) during the second year after a wildfire (fig. 12). Some of the variability of *C* is the combined uncertainty in the peak discharge and uncertainty caused by the natural variability of the rain intensity. The empirical equations are as follows: for the first year,

$$C = \frac{0.0010\Delta NBR + 0.080}{3.6};\ R^2{=}0.40, \qquad (8a)$$

and for the second year,

$$C = \frac{0.00061\Delta NBR + 0.018}{3.6};\ R^2{=}0.20. \qquad (8b)$$

The standard error (se) of estimate for both years is 0.30. The factor 3.6 converts the dimensionless value of the modified runoff coefficient, *C*, to the dimensional form having units ($m^3\ s^{-1}\ km^{-2}$) /(mm h^{-1}). The coefficient of determination for these relations suffers from the lack of data; that is, the small number of storm-runoff pairs in both years—a common problem with "natural experiments." The empirical equation 8a can be substituted into equation 7a or 7b to give an analytical expression for predicting postwildfire unit peakdischarges or peak discharges at level 2 (fig. 13). The analytical equations 8a for unit peak discharge of the first year after the wildfire are plotted in figure 13 for values of Δ*NBR* equal to 100, 300, 500, 700, and 900.

Dependence of Modified Runoff Coefficient on Hydraulic Functional Connectivity

The dependence of the modified runoff coefficient on hydraulic functional connectivity also decreases with time since the wildfire (fig. 14). These relations are more discriminating in that the data points are spread out and less clustered than for the Δ*NBR* relations.

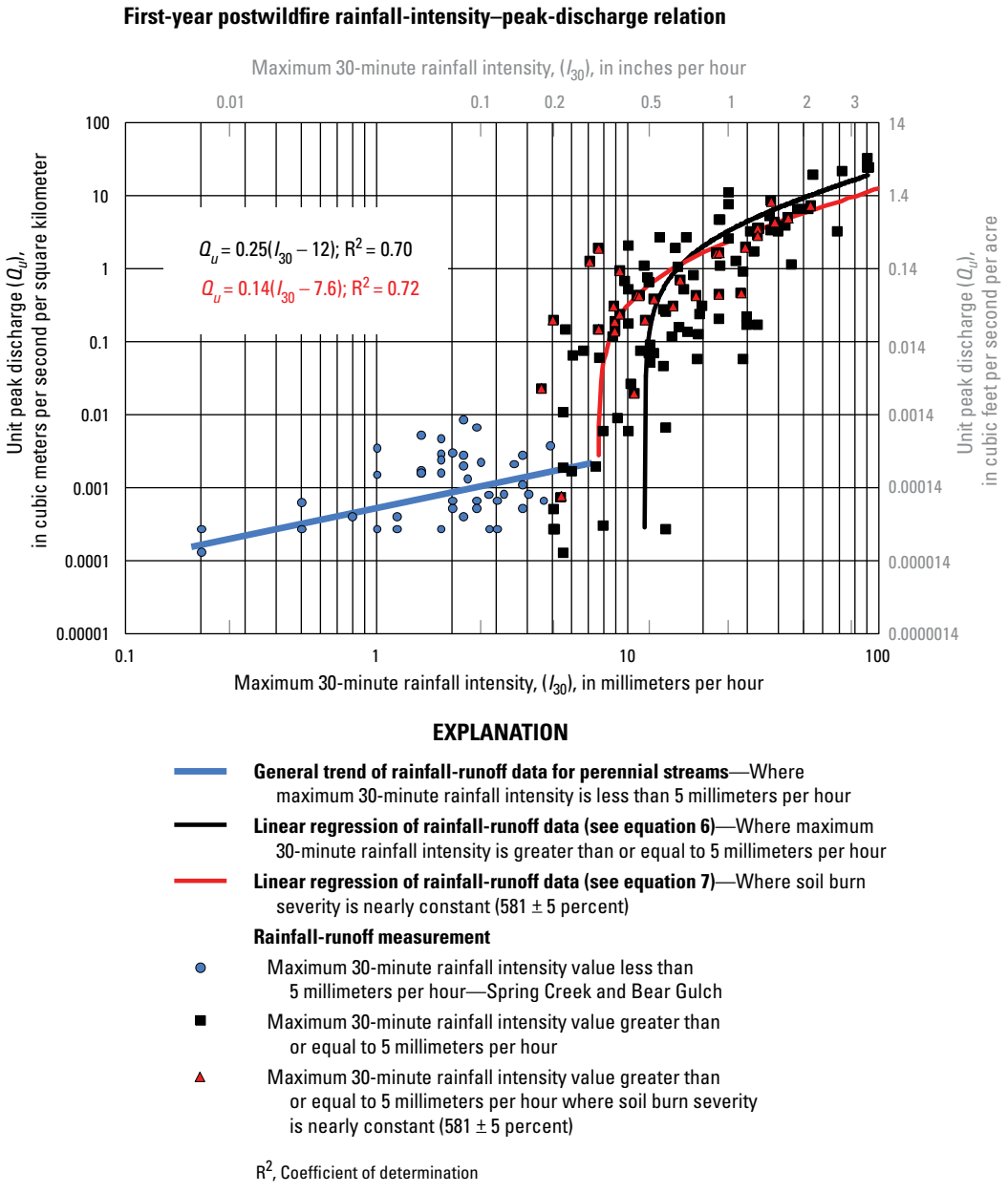

Figure 11. First-year postwildfire relation between rain intensity and peak discharge. General relation between rain intensity and unit peak discharge based on 19 basins within areas burned by eight wildfires for year of and for first year after wildfire.

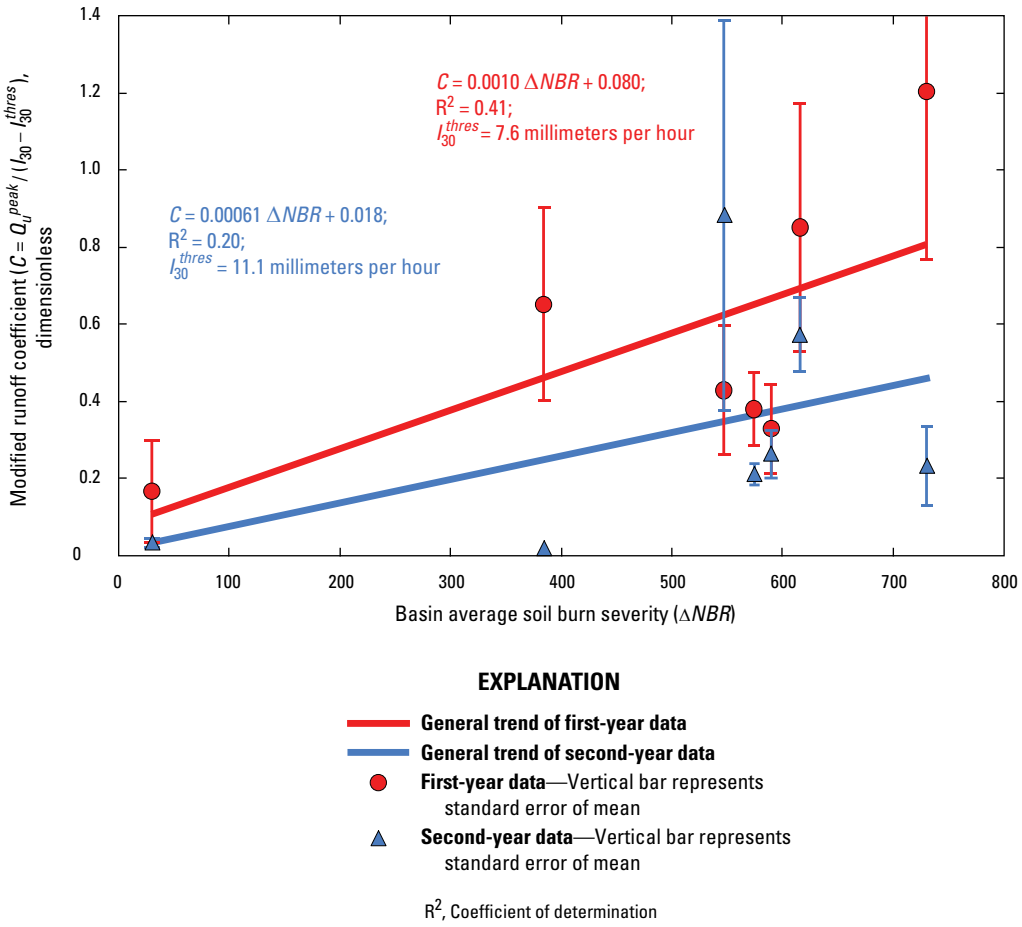

Figure 12. Dependence of modified runoff coefficient, *C*, on basin average soil burn severity metric Δ*NBR*. Data for first year after wildfire contains a few data pairs for the year of the wildfire.

$$C = \frac{0.000108\Phi + 0.14}{3.6}\text{; first year} \qquad (9a)$$

$$C = \frac{0.000085\Phi - 0.019}{3.6}\text{; second year} \qquad (9b)$$

A reduction in variance is explained by the linear regression equation compared with those equations for Δ*NBR* (fig. 12) from R^2=0.41 to 0.50 for the first year and from R^2=0.20 to 0.40 for the second year after the wildfire (fig. 14). The empirical equation 9a can be substituted into equation 7a or 7b to give an analytical expression for predicting postwildfire unit peak discharges or peak discharge at level 3 (fig. 15). Examples of the analytical expressions and curves for the unit peak discharge for the first year after the wildfire are shown on figure 15 for values of Φ equal to 100, 500, 2,000, 4,000 and 8,000. The empirical equations 8b and 9b relating the modified runoff coefficient to Δ*NBR* and Φ also can be used in the general rain intensity–peak discharge relation for the second year after the wildfire.

General Rain-Intensity–Peak-Discharge Relation for Second Year after a Wildfire

The relation for the second year after a wildfire is based on fewer data pairs and has more variability than the relation for the first year after a wildfire. The linear regression for all second-year data appears to provide an approximate upper bound,

$$Q_u = 0.077(I_{30} - 6.9);\ R^2=0.28 \qquad (10)$$

for unit peak discharges such that most values are less than those predicted by the curve in figure 16. Second-year data corresponding to the four subbasins with nearly the same

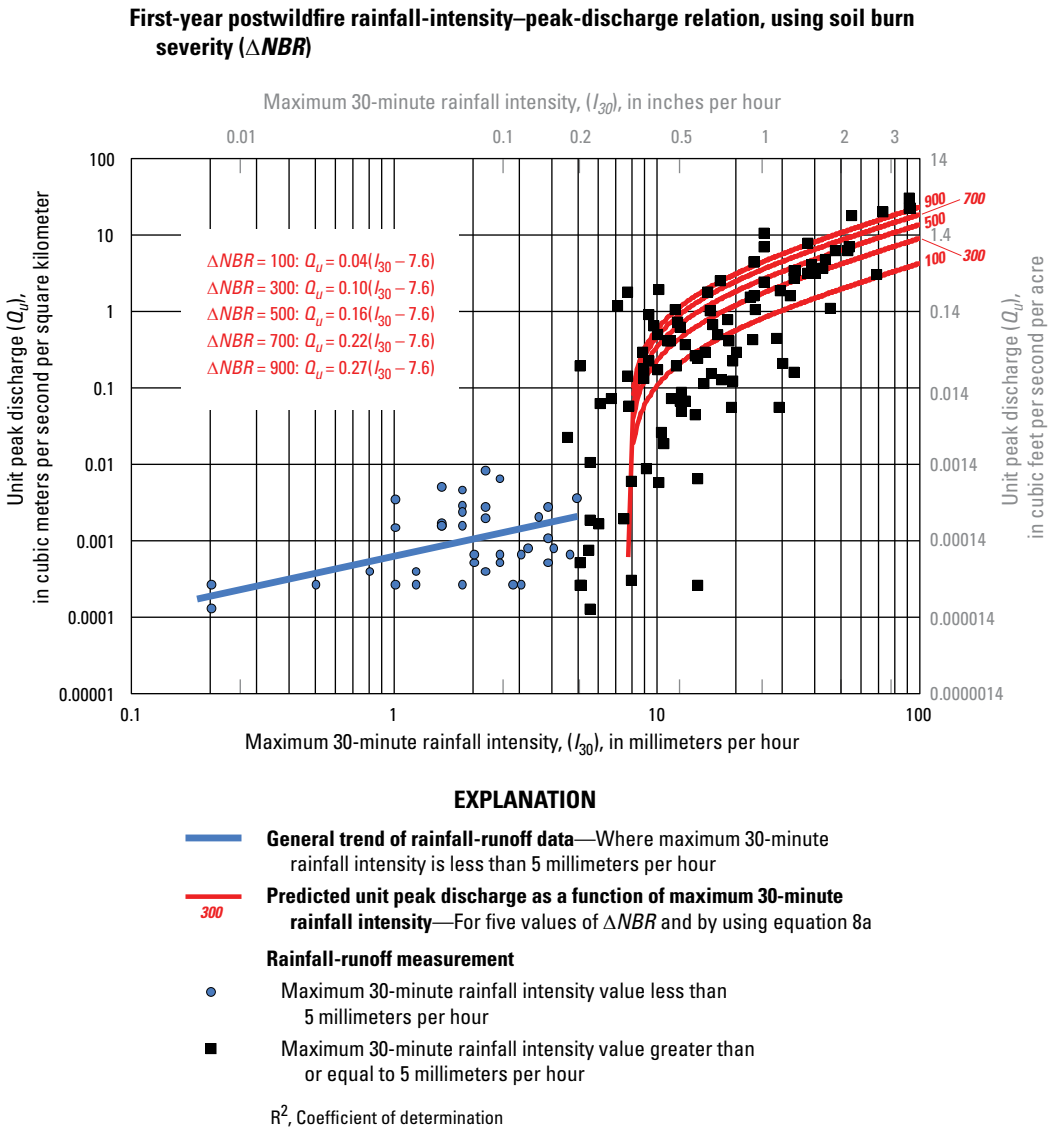

Figure 13. General first-year-postwildfire relation between rain intensity and unit peak discharge for five values of ΔNBR.

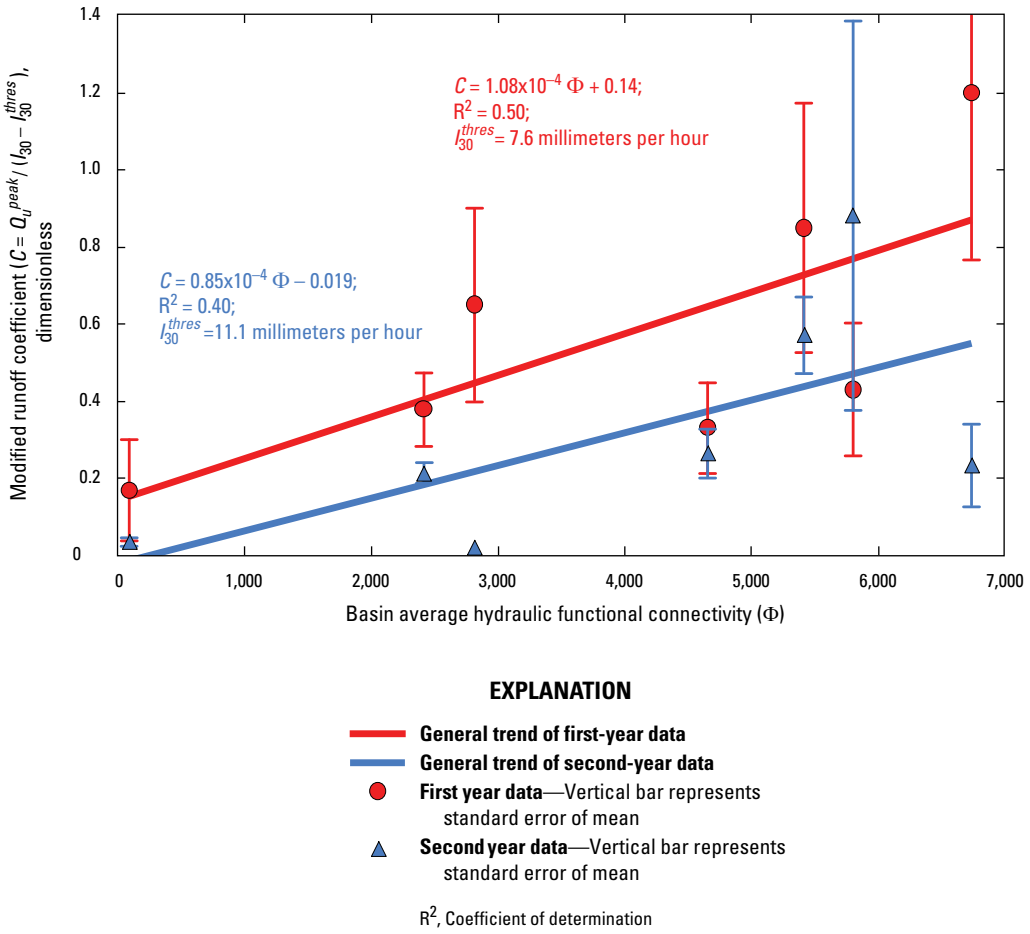

Figure 14. Dependence of the modified runoff coefficient, *C*, on basin average hydraulic functional connectivity, Φ. First-year data contain a few data pairs for the year of the wildfire.

ΔNBR (581±5 percent) provide a better linear regression equation (based on R^2 values) having the same form as those in equation 6 above:

$$Q_u = C(I_{30} - I_{30}^{thres}) , \quad (11a)$$

or in terms of the peak discharge Q [$m^3\ s^{-1}$],

$$Q = C(I_{30} - I_{30}^{thres})A , \quad (11b)$$

where C=0.12 $m^3\ s^{-1}\ km^{-2}\ mm^{-1}\ h$, I_{30}^{thres}=11.1 mm h^{-1} (0.44 in. h^{-1}), and R^2=0.52 (see appendix for more detailed regression statistics for second-year data).

Comparison with Predictions Based on Curve Number Method

The analytical method is based on rainfall and discharge data collected from many burned basins in different rainfall regimes in the western United States, so that it is a general method that can be applied to other wildfires. The 2010 Fourmile Canyon fire west of Boulder, Colo., destroyed 169 private homes in September 2010 (Fourmile Emergency Stabilization Team, 2010). Little rain fell during the fall, a continuation of a late-summer drought that provided ideal conditions for burning, but no postwildfire flooding materialized. However, postwildfire flooding became a concern for land and emergency managers who anticipated the approaching

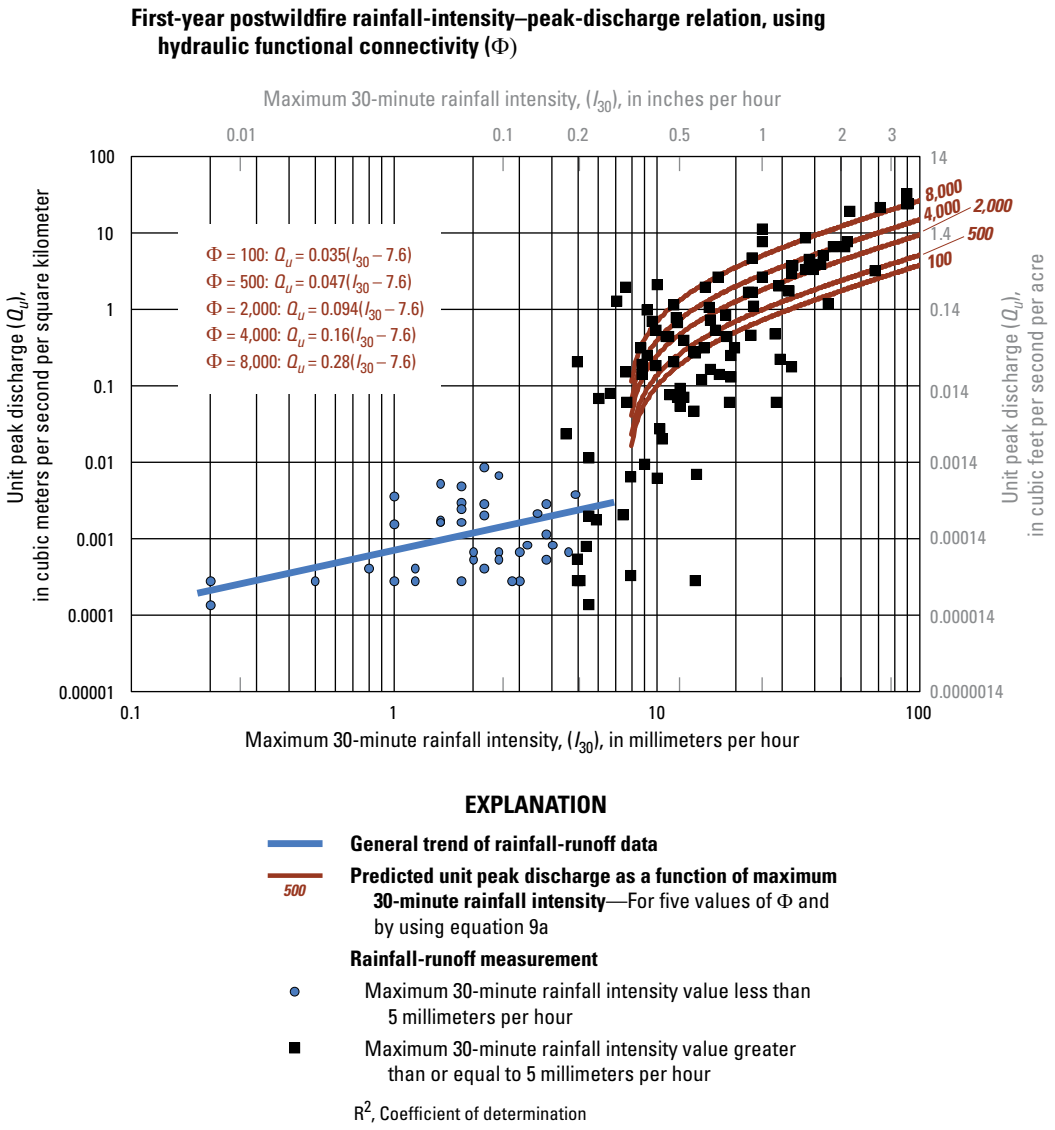

Figure 15. General first-year-postwildfire relation between rain intensity and unit peak discharge for five values of hydraulic functional connectivity.

spring rainy season with its associated frontal storms and the summer season with its typical convective storms. To plan for such postwildfire flooding, Boulder County and the Urban Drainage and Flood Control District (Denver, Colo.) solicited postwildfire flood predictions from four consultants (Vieux & Associates, Leonard Rice Engineers, Wright Water Engineers, and James Guo at University of Colorado-Denver) who used combinations of the curve number method and numerical models. Some consultants predicted peak discharge for groups of basins, whereas Wright Water Engineers (2011) predicted peak discharge for individual basins (Urban Drainage and Flood Control District (Denver, Colo.), 20011b) as well as for larger basins that included the individual basins. Predictions for the individual basins were ideal for comparison with predictions made by using the analytical method described in this report, which is based on basins of about the same drainage area (tables 1 and 2). Wright Water Engineers (2011) used the curve number loss method coupled with a particular computer model (the Hydrologic Engineering Center–hydrologic modeling system) to predict the unit peak discharges for several basins burned by the 2010 Fourmile Canyon fire. In addition, two burn severity conditions (moderate burn severity,

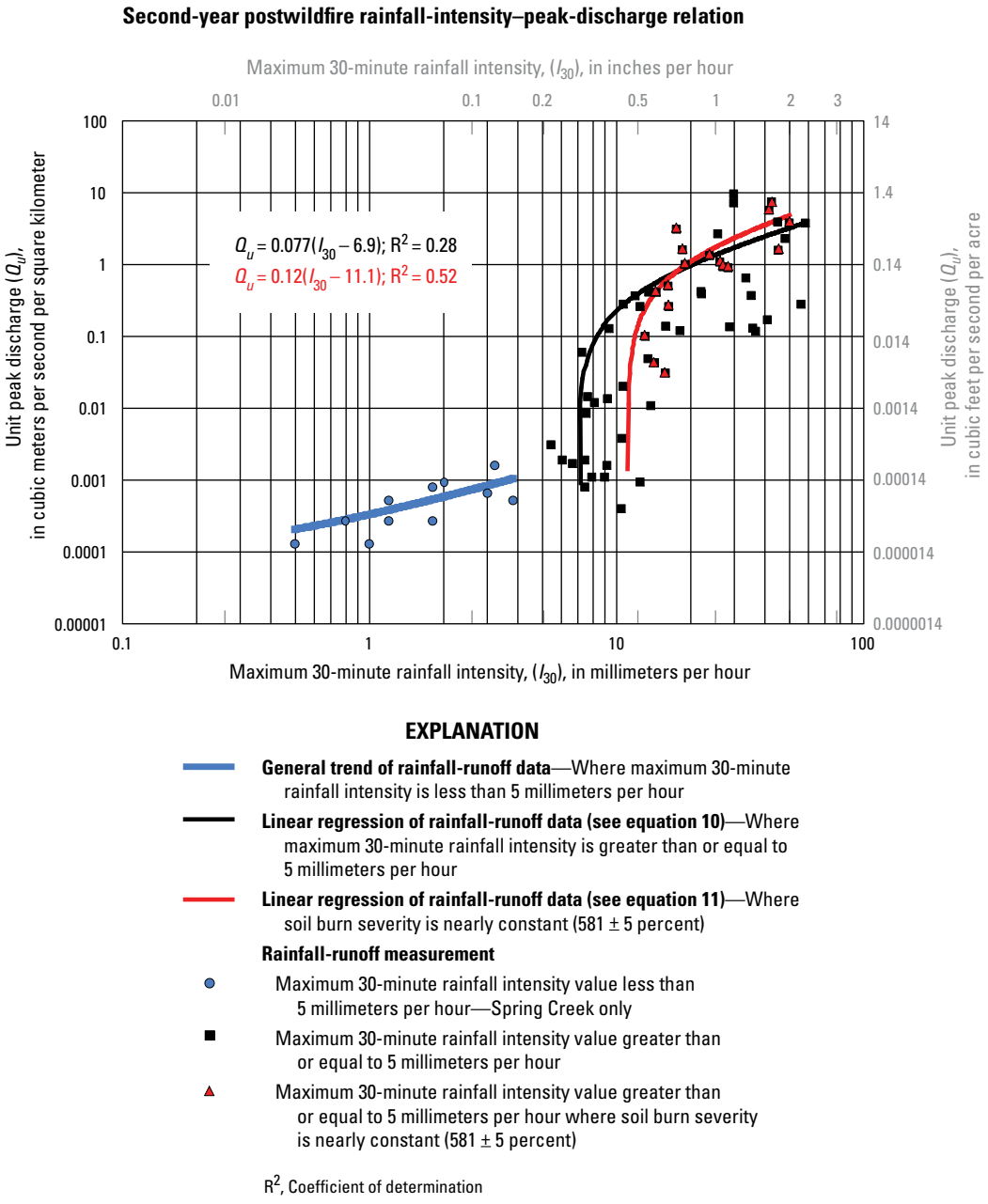

Figure 16. Second-year-postwildfire general relation between rain intensity and unit peak discharge.

Table 2. Selected characteristics of five basins burned in the 2010 Fourmile Canyon fire, Colorado.

[km², square kilometer; ha, hectare; mi², square mile; Δ*NBR*, difference (preburn minus postburn) in normalized burn ratio]

Basin	Basin number[1]	Basin area				Basin number[2]	Soil burn severity	
		(km²)	(ha)	(acre)	(mi²)		Basin average Δ*NBR*	Coefficient of variation
Emerson Gulch	10	1.16	116	287	0.45	4	585	0.37
Schoolhouse Gulch	11	0.58	58	144	0.23	5	590	0.26
Melvina Gulch	12	0.52	52	129	0.20	6	535	0.25
Unnamed tributary	16	0.44	44	109	0.17	7	530	0.19
Nancy Mine Gulch	18	0.34	34	85	0.13	8	560	0.22

[1]Ruddy and others (2010).

[2]Wright Water Engineers (2011), their figures 3, 4.

CN=89, and high burn severity, CN=96) were modeled to provide a lower and upper bound for predictions of postwildfire unit peak discharge. Their results for five burned basins (table 3; fig. 17) that are tributaries to Fourmile Creek were compared with values predicted by the analytical method using level 2 analysis (basin area and basin average Δ*NBR*). Wright Water Engineers predicted postwildfire unit peak discharges for four possible 1-hour rain intensity scenarios corresponding with 2-, 10-, 25-, and 100-year recurrence intervals. These intensities were converted to equivalent 30-minute maximum rainfall intensities (table 3) and plotted on figure 18 with the corresponding unit peak discharge (scaled from bar graphs, figs. 3.1–3.4 and 4.1–4.4, in Wright Water Engineers, 2011) to show the family of soil burn-severity curves (fig. 18).

Values of the soil burn severity metric, Δ*NBR,* for the area burned by the 2010 Fourmile Canyon fire were derived from a Landsat postwildfire image collected on 25 September 2010 and a prewildfire image collected on 21 August 2009 (R. McKinley, USGS, written commun., 2010). Basin-average soil burn severities for the five basins fell in a relatively narrow range as compared with the possible range of Δ*NBR*. The average values of Δ*NBR* for the five basins ranged from 530 to 590 (table 2); the average values for the 2000 Cerro Grand fire ranged from 30 to 730 (fig. 3*A*). This narrow range may reflect the fact that, in these generally south-facing basins, tree density (largely Ponderosa pine, *Pinus ponderosa*) is typically less than in north-facing basins. For example, within an unnamed tributary (basin 16, table 2 and fig. 17), a subbasin facing northeast is covered by Douglas fir (*Pseudotsuga menziesii*); values of Δ*NBR* ranged from 500 to 900, whereas in a more south-facing subbasin in basin 16 the values ranged from 300 to 650 (the basin average Δ*NBR* was 530). Unit peak discharge values predicted by level 2 of the analytical method (1:1 line in fig. 19) compare well with the Wright Water Engineers (2011) unit peak discharge values for moderate burn-severity conditions, but their unit peak discharges values for high burn-severity conditions are approximately twice those predicted by the analytical method. However, high burn-severity values (Wright Water Engineers, 2011) were meant to provide a worst-case scenario for planning purposes, whereas the analytical method predicts a defensible value based on measurements from burned basins.

The analytical method is easier to use than numerical computer methods, and it can be readily implemented in a relatively short time by using spreadsheet software. It is not intended to route peak discharges downstream through a stream network. It is best used to calculate peak discharges within a large burned area by applying the method to subbasins of sizes similar to those listed in table 1 (0.25–26.8 km² (62–6,620 acres)).

Table 3. Rainstorm characteristics and predicted peak discharges for five basins burned by the 2010 Fourmile Canyon fire, Colorado.

[km², square kilometers; in. h⁻¹, inches per hour; mm h⁻¹, millimeters per hour; I_{30}, maximum 30-minute intensity; m³ s⁻¹, cubic meter per second; ft³ s⁻¹, cubic feet per second]

Basin	Area		Rainstorm, 1 hour	Rain intensity		[1]Equivalent I_{30}		Peak discharge (m³ s⁻¹)			Peak discharge (ft³ s⁻¹)		
	(km²)	(acre)		(in. h⁻¹)	(mm h⁻¹)	(in. h⁻¹)	(mm h⁻¹)	Analytical	Moderate[2]	High[2]	Analytical	Moderate[2]	High[2]
Emerson	1.16	287	2-year	[3]0.90	[3]23	1.4	36	6.0	2.6	8.1	210	92	287
			10-year	1.5	38	2.4	60	11.0	7.1	16	390	250	565
			25-year	1.7	43	2.7	68	12.7	9.5	18.9	450	335	668
			100-year	2.4	61	3.8	96	18.6	16.4	28.5	660	580	1,005
Schoolhouse	0.58	144	2-year	[3]0.90	[3]23	1.4	36	3.0	1.9	5.7	110	67	200
			10-year	1.5	38	2.4	60	5.6	5.2	11.2	200	185	395
			25-year	1.7	43	2.7	68	6.4	6.7	12.9	230	238	455
			100-year	2.4	61	3.8	96	9.4	12	19.3	330	410	680
Melvina	0.52	129	2-year	[3]0.90	[3]23	1.4	36	2.9	1.8	5.2	100	62	185
			10-year	1.5	38	2.4	60	5.3	4.8	10	190	168	362
			25-year	1.7	43	2.7	68	6.1	6.1	12	220	215	412
			100-year	2.4	61	3.8	96	8.9	10	18	310	370	620
Unnamed	0.44	109	2-year	[3]0.90	[3]23	1.4	36	2.1	1.6	4.5	74	55	160
			10-year	1.5	38	2.4	60	3.9	4.2	9.2	140	150	325
			25-year	1.7	43	2.7	68	4.5	5.4	10	160	190	370
			100-year	2.4	61	3.8	96	6.6	9.3	15	230	330	535
Nancy Mine	0.34	85	2-year	[3]0.90	[3]23	1.4	36	1.7	1.1	3.5	60	40	123
			10-year	1.5	38	2.4	60	3.1	3.4	7.1	110	120	250
			25-year	1.7	43	2.7	68	3.6	4.2	7.9	130	150	280
			100-year	2.4	61	3.8	96	5.3	7.2	12	190	255	420

[1]30-minute rainfall depths are converted to equivalent 1-hour intensities by multiplying by 0.79 (Miller and others, 1973, their table 12) and then by 2.

[2]Source: Wright Water Engineers (2011).

[3]This value differs from the value (0.79 in. h⁻¹) derived from NOAA Atlas 2, v. III—Colorado (Miller and others, 1973) and from the value (0.75 in. h⁻¹) reported in Criteria Manual of the Urban Drainage and Flood Control District (Urban Drainage and Flood Control District (Denver, Colo.), 2004). This value is used in this report for comparison purposes only.

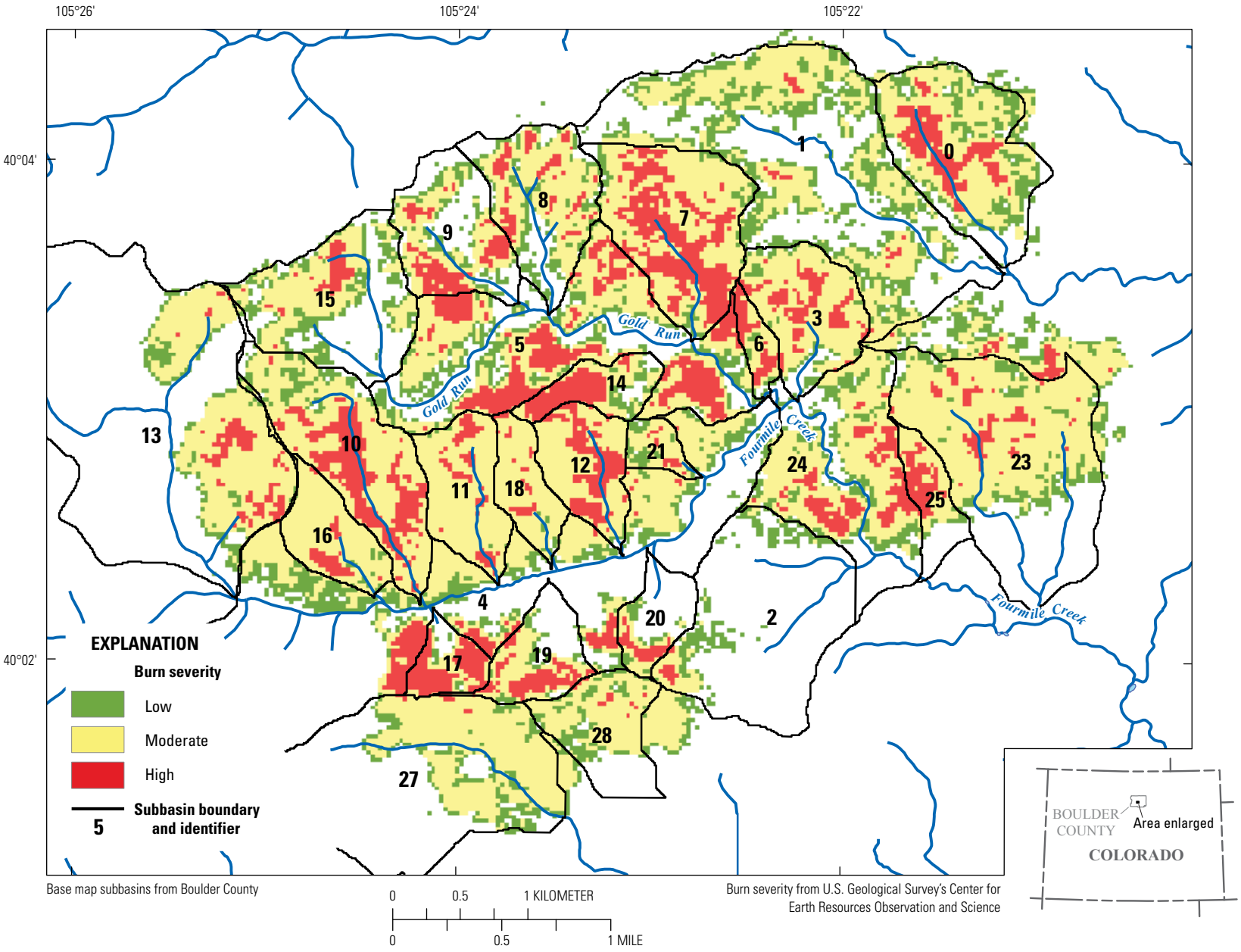

Figure 17. Qualitative categories of burn severity in a mountainous area, Fourmile Canyon (near Boulder, Colorado) burned by the 2010 Fourmile Canyon fire. Prepared by Sheila Murphy. Subwatersheds provided by Boulder County, Colorado; burn severity from U.S. Geological Survey Earth Resources Observation and Science Center.

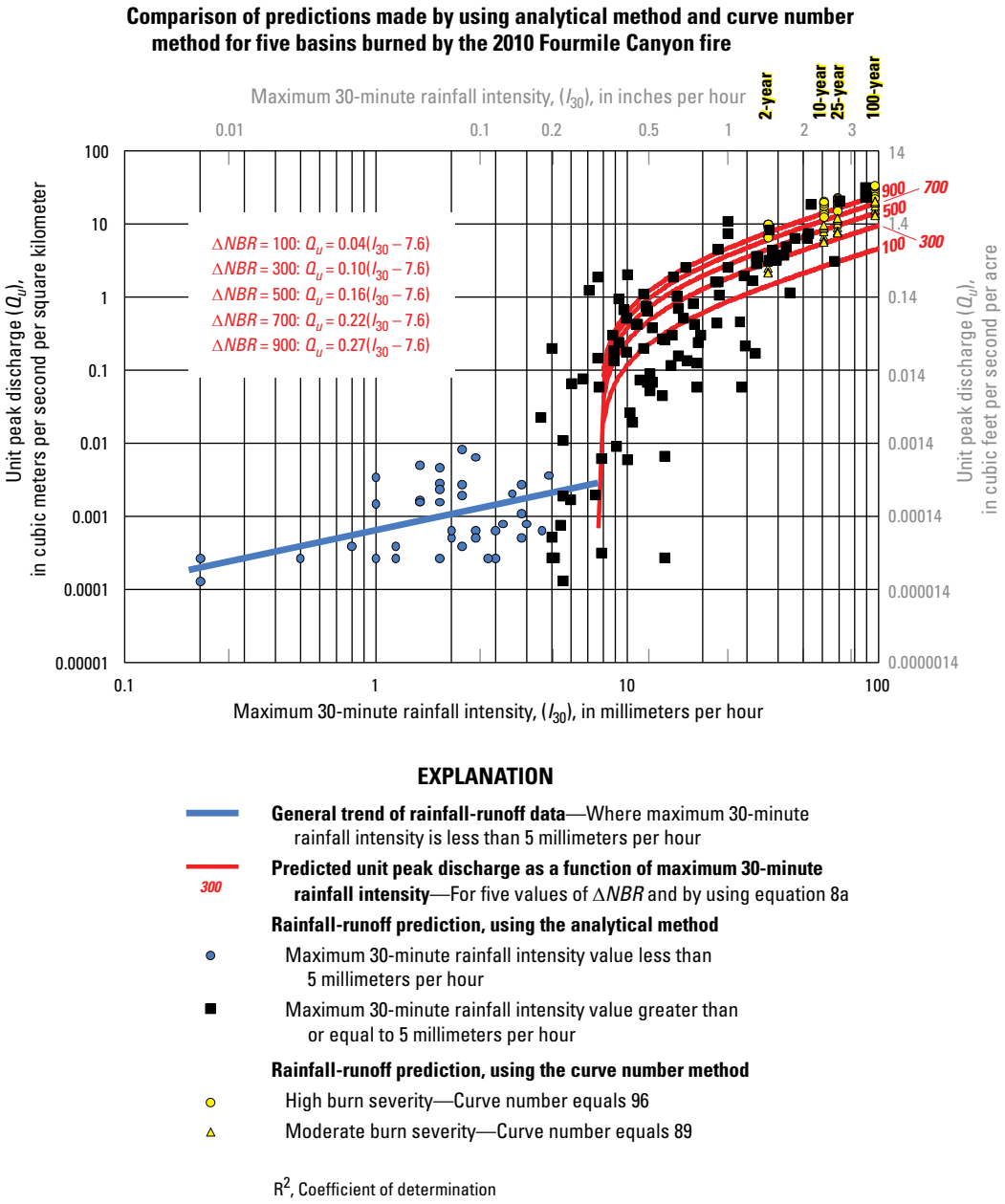

Figure 18. Predictions by analytical method and by curve number method of unit peak discharge as a function of rain intensity in five basins burned by 2010 Fourmile Canyon fire, Colorado (see fig. 17 for locations). Curve number predictions generated for four possible 1-hour rainstorms with recurrence intervals of 2, 10, 25, and 100 years (Wright Water Engineers, 2011).

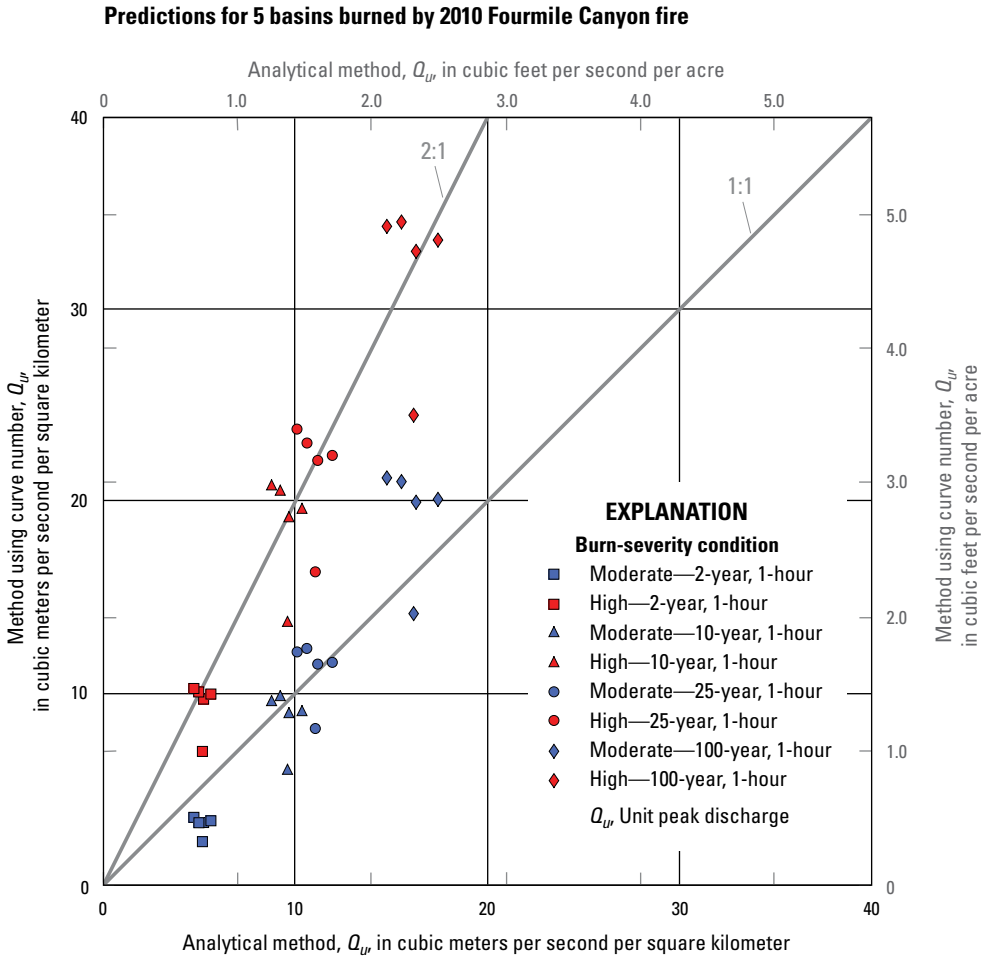

Figure 19. Comparison of predictions of unit peak discharge made by the analytical method and by the curve number method for five basins burned by Fourmile Canyon fire, Colorado, for 1-hour rainstorms with four recurrence intervals.

Summary

Paired field measurements of the unit peak discharge, Q_u, from burned basins encompass 6 orders of magnitude, whereas the associated values of I_{30} encompass only about 1 order of magnitude. These magnitudes indicate the extreme sensitivity of postwildfire peak discharge to rain intensity. An analytical method was developed to predict postwildfire peak discharge based on these natural pairs of rainfall and runoff measurements from actual burned basins. By using natural pairs of rainfall and runoff, the analytical method retains the cause-and-effect relation, whereas other methods, such as the curve number method, do not. The analytical method is applied to predict postwildfire peak discharges for selected basins burned by a wildfire in 2010, and these analytical predictions are compared with numerical computer predictions for the same basins.

Empirical equations to determine peak discharge for the year of a wildfire or for the first year after a wildfire take one of two forms: For the level 1 analysis, the modified runoff coefficient C=0.24 $m^3\ s^{-1}\ km^{-2}\ mm^{-1}\ h$ is used. For level 2 or 3 analysis, C is replaced by relations for change in normalized burn ratio (ΔNBR) or hydraulic functional connectivity (Φ). In the following equations, Q (in units of $m^3\ s^{-1}$) is the peak discharge, I_{30} (in units of mm h^{-1}) is maximum 30-minute rain intensity, and A (in units of km^2) is basin area.

Level 1: $Q = 0.24(I_{30} - 12) \cdot A$

Level 2: $Q = [\frac{0.0010\Delta NBR + 0.080}{3.6}](I_{30} - 7.6) \cdot A$

Level 3: $Q = [\frac{0.000108\Phi + 0.14}{3.6}](I_{30} - 7.6) \cdot A \cdot$

The factor of 3.6 converts the dimensionless value of the modified runoff coefficient, C, to the dimensional form in

units of (m^3 s^{-1} km^{-2})/(mm h^{-1}). If necessary, similar relations can be derived using inch-pound units, or the final value of Q in cubic meters per second can be converted to cubic feet per second.

Empirical equations for the peak discharge during the second year after a wildfire use C=0.12 m^3 s^{-1} km^{-2} mm^{-1} h for level 1 analysis, and relations for ΔNBR and Φ for levels 2 and 3 analysis. The relations are as follows:

Level 1: $Q = 0.12(I_{30} - 11) \cdot A$

Level 2: $Q = [\frac{0.00061\Delta NBR + 0.18}{3.6}](I_{30} - 11) \cdot A$

Level 3: $Q = [\frac{0.000085\Phi - 0.02}{3.6}](I_{30} - 11) \cdot A$.

The unit peak discharge response shows an abrupt change at I_{30}≈5 mm h^{-1}; this threshold of I_{30} may relate to a change in runoff generation process from saturated-excess to infiltration-excess overland flow. Linear regression analysis of all the data gave estimated values of I_{30}^{thres}=7.6 mm h^{-1} for the year of the wildfire and the following first year after the wildfire and 11 mm h^{-1} for the second year after the wildfire. A second estimate of I_{30}^{thres}, based on no-discharge responses in the ephemeral basins of Rendija Canyon, was 7.7 mm h^{-1} (0.30 in. h^{-1}) and was essentially identical to the value for the first year.

In using any of these empirical equations developed from natural pairs of rainfall and peak discharge measurements, the associated uncertainty needs to be kept in mind. This uncertainty (coefficient of determination values are shown on appropriate figures, and additional regression statistics are listed in the appendix) is inherent in the natural variability of rain intensity and the variability of peak discharge measurements made in high-energy environments associated with postwildfire floods.

The analytical method is easier to use than numerical computer methods, and it can be readily implemented in a relatively short time by using spreadsheet software. It is not intended to route peak discharges downstream through a stream network. It is best used to calculate peak discharges within a large burned area by applying the method to subbasins of sizes similar to those listed in table 1 (0.25–26.8 km^2 (62–6,620 acres)).

Acknowledgments

Data collection was possible only with the field help of Erica Bigio, Joe Gartner, John Gartner, and Brian Ragan. Deborah Martin provided not only field assistance but also valuable discussions in the field and in the office. Data for the Galena fire in South Dakota were provided by Dan Driscoll, who also provided many insights into wildfire in that climatic regime. The report is now better balanced because of thorough reviews by Brian Ebel and Bob Jarrett, who had different perspectives.

References Cited

Baltas, E.A., Dervos, N.A., and Mimikou, M.A., 2007, Technical note—Determination of the SCS initial abstraction ratio in an experimental watershed in Greece: Hydrology and Earth System Sciences, v. 11, p. 1825–1829.

Bauer, Kurt, 2011, Memorandum to flood preparedness support staff by Utilities Project Manager, City of Boulder Public Works Department, Boulder County, Colo., 3 p.

Beven, K.J., 2001, Rainfall-runoff modelling—The primer: New York, John, 353 p.

Beven, K.J., and Kirkby, M.J., 1979, A physically based, variable contributing area model of basin hydrology: Hydrological Sciences Bulletin, v. 24, p. 43–69.

Chorley, R.J., 1978, The hillslope hydrological cycle, *in* Hillslope hydrology: Kirkby, M.J. (ed.), London, John Wiley, 142 p.

Chow, V.T., 1964, Runoff, *in* Handbook of applied hydrology: Chow, V.T. (ed.), New York, McGraw-Hill, ch. 14, 54 p.

Copeland, O.L., Jr., and Croft, A.R., 1962, The Dog Valley flood of August 12, 1961 [abs.]: Journal of Geophysical Research, v. 67, no. 4, p. 1633.

DeBano, L.F., 2000, The role of fire and soil heating on water repellency in wildland environments—A review: Journal of Hydrology, v. 231/232, p. 195–206.

Doerr, S.H., Shakesby, R.A., and Walsh, R.P.D., 2000, Soil water repellency—Its causes, characteristics and hydrogeomorphological significance: Earth-Science Reviews, v. 51, p. 33–65.

Dunne, Thomas, and Black, R.D., 1970, Partial area contributions of storm runoff in a small New England watershed: Water Resources Research, v. 6, p. 1296–1311.

Dunne, Thomas, and Leopold, L.B., 1978, Water in environmental planning: New York, W.H. Freeman, 818 p.

Foltz, R.B., Robichaud, P.R., and Hakjun, R., 2009, A synthesis of post-fire road treatments for BAER teams—Methods, treatment effectiveness, and decisionmaking tools for rehabilitation: Fort Collins, Colo.: U.S. Department of Agriculture Forest Service Rocky Mountain Research Station, General Technical Report RMRS–GTR–228, 152 p.

Fourmile Emergency Stabilization Team, 2010, Burn severity by subwatershed (Fourmile Canyon, Boulder County, Colo.): map last accessed 7 July 2011 at *http://www.bouldercounty.org/find/library/environment/burnseveritybywatershed11x17.pdf*

Giovannini, Giacomo, Lucchesi, S., and Giachetti, M., 1988, Effect of heating on some physical and chemical parameters related to soil aggregation and erodibility: Soil Science, v. 146, no. 4, p. 255–261.

Helsel, D.R., and Hirsch, R.M., 1992, Statistical methods in water resources—Studies in environmental science 49: New York, Elsevier, 529 p.

Hirschboeck, K.K., 1991, Climate and floods, *in* Paulson, R.W., Chase, E.B., Roberts, R.S., and Moody, D.W. (compilers), National water summary 1988–89. Hydrologic events and floods and droughts: U.S. Geological Survey Water-Supply Paper 2375, p. 67–88.

Horton, R.E., 1933, The role of infiltration in the hydrologic cycle: Transactions, American Geophysical Union, v. 14, p. 446–460.

Jarrett, R.D., 2001, Paleohydrologic estimates of convective rainfall in the Rocky Mountains, *in* Precipitation Extremes—Prediction, Impacts and Responses Symposium, Albuquerque, N. Mex., January 14–18, 2001: American Meteorological Society, p. J40–J43.

Jiang, Ruiyun, 2001, Investigation of the runoff curve number initial abstraction ratio: Tucson, University of Arizona, Masters thesis, 120 p.

Key, C.H., and Benson, N.C., 2004, Landscape assessment—Remote sensing of severity, the normalized burn ratio; and ground measure of severity, the composite burn index, *in* Lutes, D.C., Keane, R.E., Caratti, J.F., and others (eds.), FIREMON—Fire effects monitoring and inventory system: Ogden, Utah, U.S. Department of Agriculture Forest Service Rocky Mountain Research Station, General Technical Report RMRS–GTR–164–CD, p. LA1–55.

Kincer, J.B., 1919, The seasonal distribution of precipitation and its frequency and intensity in the United States: Monthly Weather Review, September, p. 624–631.

Krammes, J.S., and Rice, R.M., 1963, Effect of fire in the San Dimas Experimental Forest, *in* Arizona Watershed Symposium, 7th, Phoenix, Ariz., September 18, 1963, Proceedings, p. 31–34.

Kunze, M.D., and Stednick, J.D., 2006, Streamflow and suspended sediment yield following the 2000 Bobcat fire, Colorado: Hydrological Processes, v. 20, p. 1661–1681.

Livingston, R.K., and Minges, D.R., 1987, Techniques for estimating regional flood characteristics of small rural watersheds in the Plains region of eastern Colorado: U.S. Geological Survey Water-Resources Investigations Report 87–4094, 72 p.

Miller, J.F., Frederick, R.H., and Tracey, R.J., 1973, NOAA atlas 2. Precipitation-frequency atlas of the western United States, v. III—Colorado: U.S. Department of Commerce, National Oceanic and Atmospheric Administration National Weather Service, 67 p.

Mockus, Victor, 1949, Estimation of total (and peak rates of) surface runoff for individual storms: U.S. Department of Agriculture Soil Conservation Service, 51 p.

Mockus, Victor, 1972, Estimation of direct runoff from storm rainfall, section 4 (Hydrology), ch. 10, *in* National Engineering Handbook: U.S. Department of Agriculture Soil Conservation Service, 23 p.

Moody, J.A., and Martin, D.A., 2001a, Post-fire, rainfall intensity–peak discharge relations for three mountainous watersheds in the western USA: Hydrological Processes, v. 15, p. 2981–2993.

Moody, J.A., and Martin, D.A., 2001b, Hydrologic and sedimentologic response of two burned watersheds in Colorado: U.S. Geological Survey Water-Resources Investigation Report 01–4122, 142 p.

Moody, J.A., and Martin, D.A., 2009, Synthesis of sediment yields after wildland fire in different rainfall regimes in the western United States: International Journal of Wildland Fire, v. 18, p. 96–115.

Moody, J.A., Martin, D.A., and Cannon, S.H., 2008b, Post-wildfire erosion response in two geologic terrains in the western USA: Geomorphology, 95, p. 103–118.

Moody, J.A., Martin, D.A., Haire, S.L., and Kinner, D.A., 2008a, Linking runoff response to burn severity after a wildfire: Hydrological Processes, v. 22, p. 2063–2074.

Moody, J.A., Martin, D.A., Oakley, T.M., and Blanken, P.D., 2007, Temporal and spatial variability of soil temperature and soil moisture after a wildfire: U.S. Geological Survey Scientific Investigations Report 2007–5015, 89 p.

Osborne, H.B., and Renard, K.G., 1970, Thunderstorm runoff on the Walnut Gulch experimental watershed, Arizona, USA, *in* The results of research on representative and experimental basins, v. 1. IAHS-UNESCO symposium, Wellington, New Zealand, December 1970, Proceedings: International Association of Hydrological Sciences publication 96, p. 455–464.

Parsons, Annette, Robichaud, P.R., Lewis, S.A., Napper, C., and Clark, J.T., 2010, Field guide for mapping post-fire soil burn severity: U.S. Department of Agriculture Forest Service Rocky Mountain Research Station, General Technical Report RMRS–GTR–243, 49 p.

Reneau, S.L., and Kuyumjian, G.A., 2004, Rainfall-runoff relations in Pueblo Canyon, New Mexico, after the Cerro Grande fire: Los Alamos National Laboratory Report LA–UR–04–8810, 32 p.

Ruddy, B.C., Stevens, M.R., Verdin, K.L., and Elliott, J.G., 2010, Probability and volume of potential postwildfire debris flows in the 2010 Fourmile burn area, Boulder County, Colorado: U.S. Geological Survey Open-File Report 2010–1244, 5 p.

San Dimas Staff, 1954, Fire-flood sequences on the San Dimas Experimental Forest: U.S. Department of Agriculture California Forest and Range Experiment Station Technical Paper 6, 29 p.

Sinclair, J.D., and Hamilton, E.L., 1955, Streamflow reactions of a fire-damaged watershed: American Society of Civil Engineers Hydraulic Division, 81, Proceedings, separate 629, p. 1–17.

Smith, D.M., 1994, The forests of the United States, *in* Regional silviculture of the United States (3d ed.): Barrett, J.W. (ed.), New York, John Wiley, p. 1–30.

Snider, Dean, 1972, Hydrographs, *in* National engineering handbook: U.S. Department of Agriculture Soil Conservation Service, section 4, ch. 16, 26 p.

Urban Drainage and Flood Control District (Denver, Colo.), 2004, Rainfall, *in* Urban Drainage and Flood Control District (Denver, Colo.) criteria manual, v. 1, ch. 4, 27 p., accessed 23 April 2011 at *http://www.udfcd.org/downloads/down_critmanual.htm*

Urban Drainage and Flood Control District (Denver, Colo.), 2011a, Flash flood prediction program: Accessed 23 April 2011 at *http://f2p2.udfcd.org/*

Urban Drainage and Flood Control District (Denver, Colo.), 2011b, Fourmile Creek flood risk assessment: Urban Drainage and Flood Control District (Denver, Colo.), last updated 18 March 2011. *http://www.udfcd.org/resources/pdf/conferences/conf2011/3_Post-Fire_Flood_Risk_Assessment.pdf*.

Woodward, D.E., Hawkins, R.H., Jiang, R., Hjelmfelt, A.T. Jr., and Van Mullem, J.A., 2003, Runoff curve number method—Examination of the initial abstraction ratio: World Water & Environmental Resources Congress 2003, Philadelphia, Pa., 23–26 June 2003, Proceedings, p. 1–10.

Wright Water Engineers, 2011, Summary of findings—Fourmile Canyon post-fire hydrology and discussion of conceptual mitigation measures: Wright Water Engineers Memorandum, 20 January 2011, Denver, Colo., 9 p. plus figures.

Appendix

Appendix. Rain Intensities and Unit Peak Discharges for Year of a Wildfire and the First and Second Years after a Wildfire.

[There was insufficient data for all the rainfall regimes to justify listing and determining general regression relations for the third and fourth years after wildfire. I_{30}, maximum 30-minute intensity; Q_u, water discharge per unit area; yr, year; mm, millimeter; h, hour; m, meter; s, second; km, kilometer; ft, feet; CA, California; NV, Nevada]

First year data						Second year data					
Basin	Time since fire (yr)	I_{30} (mm h^{-1})	I_{30} (inch h^{-1})	Q_u, unit peak discharge ($m^3\ s^{-1}\ km^{-2}$)	Q_u, unit peak discharge ($ft^3\ s^{-1}\ acre^{-1}$)	Basin	Time since fire (yr)	I_{30} (mm h^{-1})	I_{30} (inch h^{-1})	Q_u, unit peak discharge ($m^3\ s^{-1}\ km^{-2}$)	Q_u, unit peak discharge ($ft^3\ s^{-1}\ acre^{-1}$)
Bobcat Gulch	0.1	42.0	1.65	3.9	0.56	Bobcat Gulch	2	8.1	0.32	0.012	0.0017
Bobcat Gulch	0.1	12.0	0.47	0.65	0.093						
Bobcat Gulch	0.1	14.0	0.55	0.26	0.037	Spring Creek	2	48.0	1.89	2.3	0.33
Jug Gulch	0.1	12.0	0.47	0.070	0.010	Spring Creek	2	44.8	1.76	3.9	0.56
						Spring Creek	2	12.4	0.49	0.00094	0.00013
						Spring Creek	2	10.4	0.41	0.00040	0.000057
Bobcat Gulch	1	10.0	0.39	0.006	0.0009	Spring Creek	2	9.1	0.36	0.0016	0.00023
Bobcat Gulch	1	12.6	0.50	0.070	0.010	Spring Creek	2	8.9	0.35	0.0011	0.00016
Jug Gulch	1	9.0	0.35	0.0090	0.0013	Spring Creek	2	7.9	0.31	0.0011	0.00016
Jug Gulch	1	11.2	0.44	0.075	0.011	Spring Creek	2	7.4	0.29	0.0019	0.00027
Bobcat Gulch	1	15.9	0.63	0.16	0.023	Spring Creek	2	7.4	0.29	0.00080	0.00011
Jug Gulch	1	12.2	0.48	0.090	0.013	Spring Creek	2	6.6	0.26	0.0017	0.00024
Jug Gulch	1	18.2	0.72	0.82	0.12						
Bobcat Gulch	1	14.8	0.58	0.12	0.017	CA-NV	1.5	29.7	1.17	7.2	1.0
Jug Gulch	1	31.6	1.24	1.7	0.24	CA-NV	1.5	29.7	1.17	9.6	1.4
Bobcat Gulch	1	23.2	0.91	1.1	0.16						
Jug Gulch	1	13.8	0.54	0.046	0.0066	Bear Gulch	2	28.6	1.13	0.14	0.019
						Bear Gulch	2	36.5	1.44	0.12	0.017
Spring Creek	0.1	90.0	3.54	24	3.43	Bear Gulch	2	10.5	0.41	0.0038	0.00054
Spring Creek	1	51.9	2.04	6.6	0.94	Bear Gulch	2	13.7	0.54	0.011	0.0016
Spring Creek	1	32.4	1.28	0.17	0.024	Bear Gulch	2	10.6	0.42	0.28	0.040
Spring Creek	1	19.6	0.77	0.31	0.044	Bear Gulch	2	15.8	0.62	0.14	0.020
Spring Creek	1	19.1	0.75	0.24	0.034	Bear Gulch	2	7.6	0.30	0.014	0.0021
Spring Creek	1	14.0	0.55	0.00027	0.000039	Bear Gulch	2	13.4	0.53	0.049	0.0070
Spring Creek	1	12.2	0.48	0.052	0.0074	Bear Gulch	2	9.2	0.36	0.014	0.0019
Spring Creek	1	10.2	0.40	0.027	0.0039	Bear Gulch	2	6.0	0.24	0.0019	0.00027
Spring Creek	1	7.9	0.31	0.0061	0.0009	Bear Gulch	2	5.4	0.21	0.0031	0.00044
Spring Creek	1	7.4	0.29	0.0020	0.00029						
Spring Creek	1	6.0	0.24	0.066	0.0094	Pueblo Canyon	2	25.6	1.01	2.7	0.38
Spring Creek	1	5.9	0.23	0.0017	0.00024	Pueblo Canyon	2	11.8	0.47	0.37	0.052
Spring Creek	1	5.5	0.22	0.0019	0.00027	Pueblo Canyon	2	13.4	0.53	0.41	0.059
Spring Creek	1	5.5	0.22	0.00013	0.000019	Pueblo Canyon	2	10.6	0.42	0.020	0.0029
Spring Creek	1	5.5	0.22	0.011	0.0016	Pueblo Canyon	2	9.3	0.37	0.13	0.02
Spring Creek	1	5.1	0.20	0.00027	0.000039						
Spring Creek	1	5.0	0.20	0.00052	0.000074	Rendija Canyon 2	2	58.0	2.28	3.8	0.54

Appendix. Rain Intensities and Unit Peak Discharges for Year of a Wildfire and the First and Second Years after a Wildfire.—Continued

[There was insufficient data for all the rainfall regimes to justify listing and determining general regression relations for the third and fourth years after wildfire. I_{30}, maximum 30-minute intensity; Q_u, water discharge per unit area; yr, year; mm, millimeter; h, hour; m, meter; s, second; km, kilometer; ft, feet; CA, California; NV, Nevada]

First year data						Second year data					
Basin	Time since fire (yr)	I_{30} (mm h^{-1})	I_{30} (inch h^{-1})	Q_u, unit peak discharge ($m^3\ s^{-1}\ km^{-2}$)	Q_u, unit peak discharge ($ft^3\ s^{-1}\ acre^{-1}$)	Basin	Time since fire (yr)	I_{30} (mm h^{-1})	I_{30} (inch h^{-1})	Q_u, unit peak discharge ($m^3\ s^{-1}\ km^{-2}$)	Q_u, unit peak discharge ($ft^3\ s^{-1}\ acre^{-1}$)
Spring Creek	1	5.0	0.20	0.00027	0.000039	Rendija Canyon 2	2	12.4	0.49	0.26	0.037
						Rendija Canyon 2	2	55.7	2.19	0.28	0.040
CA-NV	0.1	39.1	1.54	3.3	0.47	Rendija Canyon 2	2	21.9	0.86	0.42	0.060
CA-NV	0.1	22.9	0.90	4.7	0.67	Rendija Canyon 2	2	22.0	0.87	0.39	0.056
CA-NV	0.1	23.0	0.91	4.7	0.67	Rendija Canyon 2	2	33.3	1.31	0.65	0.093
CA-NV	0.1	29.5	1.16	0.22	0.031						
CA-NV	0.1	18.8	0.74	0.059	0.0084	Rendija Canyon 3	2	49.9	1.96	3.8	0.54
CA-NV	0.5	89.2	3.51	24	3.43	Rendija Canyon 3	2	16.2	0.64	0.26	0.037
CA-NV	0.5	89.2	3.51	33	4.67	Rendija Canyon 3	2	14.2	0.56	0.043	0.006
						Rendija Canyon 3	2	28.2	1.11	0.90	0.13
Bear Gulch	1	7.9	0.31	0.00031	0.000044	Rendija Canyon 3	2	18.9	0.74	1.00	0.14
Bear Gulch	1	14.1	0.55	0.0067	0.0010	Rendija Canyon 3	2	16.1	0.63	0.50	0.071
Bear Gulch	1	19.0	0.75	0.13	0.0181						
Bear Gulch	1	17.2	0.68	0.14	0.0194	Rendija Canyon 4	2	40.7	1.60	0.17	0.024
Bear Gulch	1	28.5	1.12	0.059	0.01						
Bear Gulch	1	67.3	2.65	3.2	0.46	Rendija Canyon 9	2	42.3	1.67	7.4	1.1
Bear Gulch	1	6.6	0.26	0.077	0.011	Rendija Canyon 9	2	17.4	0.69	3.1	0.44
						Rendija Canyon 9	2	15.7	0.62	0.031	0.0044
Pueblo Canyon	0.1	13.8	0.54	0.27	0.039						
Pueblo Canyon	0.1	7.7	0.30	0.060	0.0085	Rendija Canyon 11	2	41.3	1.63	5.7	0.81
Pueblo Canyon	0.1	16.6	0.66	0.52	0.075	Rendija Canyon 11	2	18.4	0.72	1.6	0.23
Pueblo Canyon	0.1	9.6	0.38	0.67	0.10	Rendija Canyon 11	2	14.4	0.57	0.41	0.059
Pueblo Canyon	0.1	9.9	0.39	0.18	0.03	Rendija Canyon 11	2	23.7	0.93	1.3	0.19
Pueblo Canyon	1	46.7	1.84	6.6	0.94						
Pueblo Canyon	1	9.9	0.39	0.52	0.075	Rendija Canyon 13	2	26.9	1.06	0.93	0.13
Pueblo Canyon	1	11.5	0.45	1.1	0.16	Rendija Canyon 13	2	26.1	1.03	1.1	0.15
Pueblo Canyon	1	15.7	0.62	1.1	0.15	Rendija Canyon 13	2	13.0	0.51	0.10	0.014
Pueblo Canyon	1	11.8	0.47	0.76	0.11	Rendija Canyon 13	2	45.0	1.77	1.6	0.23
Rendija Canyon 2	0.1	17.0	0.67	2.7	0.38	Rendija Canyon 14	2	18.0	0.71	0.12	0.017
Rendija Canyon 2	1	70.4	2.77	21	3.1	Rendija Canyon 14	2	35.0	1.38	0.37	0.053
Rendija Canyon 2	1	15.3	0.60	1.9	0.27	Rendija Canyon 14	2	7.5	0.30	0.0085	0.0012
Rendija Canyon 2	1	10.0	0.39	2.1	0.30	Rendija Canyon 14	2	7.2	0.28	0.060	0.0086
Rendija Canyon 2	1	54.0	2.13	19	2.7	Rendija Canyon 14	2	35.5	1.40	0.13	0.019
Rendija Canyon 2	1	36.7	1.44	3.3	0.48						

Appendix. Rain Intensities and Unit Peak Discharges for Year of a Wildfire and the First and Second Years after a Wildfire.—Continued

[There was insufficient data for all the rainfall regimes to justify listing and determining general regression relations for the third and fourth years after wildfire. I_{30}, maximum 30-minute intensity; Q_u, water discharge per unit area; yr, year; mm, millimeter; h, hour; m, meter; s, second; km, kilometer; ft, feet; CA, California; NV, Nevada]

First year data						Second year data					
Basin	Time since fire (yr)	I_{30} (mm h^{-1})	I_{30} (inch h^{-1})	Q_u, unit peak discharge (m^3 s^{-1} km^{-2})	Q_u, unit peak discharge (ft^3 s^{-1} $acre^{-1}$)	Basin	Time since fire (yr)	I_{30} (mm h^{-1})	I_{30} (inch h^{-1})	Q_u, unit peak discharge (m^3 s^{-1} km^{-2})	Q_u, unit peak discharge (ft^3 s^{-1} $acre^{-1}$)
Rendija Canyon 2	1	44.5	1.75	1.2	0.16						
						Regression Statistics for:	$Q_u = C(I_{30} - I_{30}^{thres})$				
Rendija Canyon 3	1	52.7	2.07	7.5	1.1						
Rendija Canyon 3	1	22.3	0.88	1.7	0.24	**All First Year Data**					
Rendija Canyon 3	1	5.4	0.21	0.00076	0.00011	R^2		0.70			
Rendija Canyon 3	1	10.5	0.41	0.020	0.0028	modified C		0.25			
Rendija Canyon 3	1	38.0	1.50	4.4	0.63	Standard error C		0.016			
Rendija Canyon 3	1	10.8	0.43	0.44	0.063	I_{30}^{thres}		12			
Rendija Canyon 3	1	12.6	0.50	0.39	0.056	Standard error I_{30}^{thres}		1.8			
						Standard error Q_u		3.0			
Rendija Canyon 4	1	26.8	1.06	1.3	0.18						
Rendija Canyon 4	1	28.5	1.12	0.90	0.13	Degrees of freedom		105			
Rendija Canyon 4	1	30.4	1.20	3.3	0.47	Regression sum of squares		2,148			
Rendija Canyon 4	1	13.3	0.52	2.7	0.39	Residual sum of squares		921			
Rendija Canyon 4	1	36.4	1.43	5.2	0.74						
						Only ΔNBR + 581 for first year data					
Rendija Canyon 9	0.1	25.0	0.98	11	1.61	R^2		0.72			
Rendija Canyon 9	1	22.8	0.90	0.45	0.064	modified C		0.14			
Rendija Canyon 9	1	36.8	1.45	8.5	1.2	Standard error C		0.017			
Rendija Canyon 9	1	11.0	0.43	0.43	0.061	I_{30}^{thres}		7.6			
Rendija Canyon 9	1	15.0	0.59	0.31	0.044	Standard error I_{30}^{thres}		2.6			
Rendija Canyon 9	1	22.9	0.90	1.7	0.24	Standard error Q_u		1.2			
Rendija Canyon 9	1	5.0	0.20	0.20	0.029						
Rendija Canyon 9	1	7.6	0.30	1.9	0.28	Degrees of freedom		29			
						Regression sum of squares		105			
Rendija Canyon 11	0.1	25.0	0.98	7.6	1.1	Residual sum of squares		40			
Rendija Canyon 11	1.0	4.5	0.18	0.023	0.0033						
Rendija Canyon 11	1	43.0	1.69	5.0	0.72	**All second year data**					
Rendija Canyon 11	1	8.8	0.35	0.19	0.027	R^2		0.28			
Rendija Canyon 11	1	7.6	0.30	0.15	0.021	Modified C		0.077			
Rendija Canyon 11	1	32.9	1.30	3.6	0.52	Standard error C		0.017			
Rendija Canyon 11	1	32.5	1.28	3.6	0.52	I_{30}^{thres}		6.9			
Rendija Canyon 11	1	9.2	0.36	0.95	0.14	Standard error I_{30}^{thres}		5.5			
						Standard error Q_u		1.8			
Rendija Canyon 13	0.1	25.0	0.98	2.6	0.37						

Appendix. Rain Intensities and Unit Peak Discharges for Year of a Wildfire and the First and Second Years after a Wildfire.—Continued

[There was insufficient data for all the rainfall regimes to justify listing and determining general regression relations for the third and fourth years after wildfire. I_{30}, maximum 30-minute intensity; Q_u, water discharge per unit area; yr, year; mm, millimeter; h, hour; m, meter; s, second; km, kilometer; ft, feet; CA, California; NV, Nevada]

First year data						Second year data					
Basin	Time since fire (yr)	I_{30} (mm h^{-1})	I_{30} (inch h^{-1})	Q_u, unit peak discharge ($m^3\ s^{-1}\ km^{-2}$)	Q_u, unit peak discharge ($ft^3\ s^{-1}\ acre^{-1}$)	Basin	Time since fire (yr)	I_{30} (mm h^{-1})	I_{30} (inch h^{-1})	Q_u, unit peak discharge ($m^3\ s^{-1}\ km^{-2}$)	Q_u, unit peak discharge ($ft^3\ s^{-1}\ acre^{-1}$)
Rendija Canyon 13	1	16.0	0.63	0.71	0.10	Degrees of freedom		56			
Rendija Canyon 13	1	29.0	1.14	2.0	0.28	Regression sum of squares		66.7			
Rendija Canyon 13	1	28.0	1.10	0.47	0.067	Residual sum of squares		173			
Rendija Canyon 13	1	18.5	0.73	0.43	0.061						
Rendija Canyon 13	1	9.2	0.36	0.24	0.034	**Only $\Delta NBR + 581$ for second year data**					
Rendija Canyon 13	1	11.6	0.46	0.20	0.029	R^2		0.52			
Rendija Canyon 13	1	8.7	0.34	0.31	0.044	modified C		0.12			
Rendija Canyon 13	1	32.5	1.28	2.9	0.41	Standard error C		0.031			
Rendija Canyon 13	1	8.8	0.35	0.14	0.020	I_{30}^{thres}		11			
Rendija Canyon 13	1	7.0	0.28	1.3	0.18	Standard error I_{30}^{thres}		7.0			
						Standard error Q_u		1.5			
Rendija Canyon 14	1	22.9	0.90	0.21	0.03						
Rendija Canyon 14	1	29.5	1.16	0.17	0.02	Degrees of freedom		15			
Rendija Canyon 14	1	8.6	0.34	0.12	0.02	Regression sum of squares		36.5			
Rendija Canyon 14	1	5.6	0.22	0.15	0.02	Residual sum of squares		34.1			

Publishing support provided by
Colorado and Lafayette Publishing Service Centers